Systems/Circuits

Paraventricular Nucleus Oxytocin Subsystems Promote Active Paternal Behaviors in Mandarin Voles

Zhixiong He,[1]* **Lizi Zhang,**[1]* **Wenjuan Hou,**[1]* **Xin Zhang,**[1] (ID)**Larry J. Young,**[2,3] **Laifu Li,**[1] **Limin Liu,**[1] **Huan Ma,**[1] **Yufeng Xun,**[1] **Zijian Lv,**[1] **Yitong Li,**[1] **Rui Jia,**[1] **Jingang Li,**[1] **and** (ID)**Fadao Tai**[1]

[1]Institute of Brain and Behavioral Sciences, College of Life Sciences, Shaanxi Normal University, Xi'an 710062, China, [2]Department of Psychiatry and Behavioral Sciences, Silvio O. Conte Center for Oxytocin and Social Cognition, Center for Translational Social Neuroscience, Yerkes National Primate Research Center, Emory University, Atlanta, Georgia 30033, and [3]Center for Social Neural Networks, University of Tsukuba, Tsukuba 305-8555, Japan

Paternal care plays a critical role in the development of brain and behaviors in offspring in monogamous species. However, the neurobiological mechanisms, especially the neuronal circuit, underlying paternal care is largely unknown. Using socially monogamous male mandarin voles (*Microtus mandarinus*) with high levels of paternal care, we found that paraventricular nucleus of the hypothalamus (PVN) to ventral tegmental area (VTA) or nucleus accumbens (NAc) oxytocin (OT) neurons are activated during paternal care. Chemogenetic activation/inhibition of the PVN OT projection to VTA promoted/decreased paternal care, respectively. Chemogenetic inhibition of the PVN to VTA OT pathway reduced dopamine (DA) release in the NAc of male mandarin voles during licking and grooming of pups as revealed by *in vivo* fiber photometry. Optogenetic activation/inhibition of the VTA to NAc DA pathway possibly enhanced/suppressed paternal behaviors, respectively. Furthermore, chemogenetic activation/inhibition of PVN to NAc OT circuit enhanced/inhibited paternal care. This finding is a first step toward delineating the neuronal circuit underlying paternal care and may have implications for treating abnormalities in paternal care associated with paternal postpartum depression or paternal abuse.

Key words: dopamine; nucleus accumbens; oxytocin; paraventricular nucleus of the hypothalamus; paternal behavior; ventral tegmental area

---

Significance Statement

Paternal behavior is essential for offspring survival and development in some mammalian species. However, the circuit mechanisms underlying the paternal brain are poorly understood. We show that manipulation of paraventricular nucleus of the hypothalamus (PVN) to ventral tegmental area (VTA) oxytocin (OT) projections as well as VTA to nucleus accumbens (NAc) DA projections promote paternal behaviors. Inhibition the PVN to VTA OT pathway reduces DA release in the NAc during pup licking and grooming. PVN to NAc OT circuit is also essential for paternal behaviors. Our findings identify two new neural circuits that modulate paternal behaviors.

Introduction

Parental care providing nutrition, warmth, protection and emotional attachment, is necessary for the mental and physical development of offspring (Dulac et al., 2014). In mammals, mothers invest heavily in reproduction and are often the sole caregiver to their offspring. However, in ~5% of mammalian species, including humans, fathers also provide parental care (Kleiman and Malcolm, 1981) and the absence of the father can have adverse effects on the offspring in prairie voles (Ahern and Young, 2009; Ahern et al., 2011) and mandarin voles (He et al., 2019). Paternal support can also contribute to the mental health of the mother, including reducing depression (Bhatti et al., 2019). Although many studies highlight the importance of fathering, the neurobiological mechanisms, especially the neuronal circuit, underlying paternal care, remain poorly understood.

The neuropeptide oxytocin (OT) originating from the paraventricular nucleus of the hypothalamus (PVN) facilitates various affiliative behaviors including social attachment and parental care (Bartz, 2016; Walum and Young, 2018; Bhatti et al., 2019). Hypothalamic OT regulates maternal behavior (Rilling and Young, 2014; Maynard et al., 2018) and promotes pup retrieval behavior in females mice (Marlin et al., 2015). There is also evidence that OT may be involve in fathering in humans as well (Weisman et al., 2012; Mascaro et al., 2014). Indeed, intranasal OT increases the father's neural responses to pictures of their toddlers (Li et al., 2017). However, where and how projections of OT neurons in the brain regulates paternal behavior remains largely unknown.

One possible downstream pathway modulated by OT to control paternal behavior may be the dopamine (DA) system, which is essential for motivation and reward processing (Yang et al., 2018). In rat mothers, inactivation of ventral tegmental area (VTA) DA neuron projections disrupted pup retrieval (Numan et al., 2009). Moreover, DA receptor antagonists infused into the nucleus accumbens (NAc) impairs maternal behaviors in rats (Keer and Stern, 1999; Numan et al., 2005). Finally, DA release in NAc shell of rats is essential for maternal behaviors (Champagne et al., 2004; Shahrokh et al., 2010). In female rats, the mesolimbic DA system facilitates the motivation to approach and nurture offspring via action of OT (Numan, 2007; Numan and Young, 2016). Similarly, neural activation within the mesolimbic DA system is enhanced by OT on viewing pictures of unfamiliar crying infants in women (Gregory et al., 2015). Interestingly, infusions of OT antagonist into the VTA impairs maternal behavior in rats (Pedersen et al., 1994). DA and OT interactions in the NAc shell regulate maternal behaviors in rats (Shahrokh et al., 2010), while OT signaling in the NAc mediates alloparental care in prairie voles (Olazábal and Young, 2006a; Keebaugh and Young, 2011). OT signaling in the NAc also mediates the pair bond formation in prairie voles (Walum and Young, 2018). However, neural circuit mechanisms by which OT regulates paternal behavior remain largely unexplored. PVN OT neurons project to the VTA (Hung et al., 2017) and the NAc (Ross et al., 2009; Nardou et al., 2019). Thus, we predicted that PVN to VTA OT projections modulate paternal behaviors via the VTA to NAc DA pathway.

Using socially monogamous mandarin voles (*Microtus mandarinus*) with high levels of paternal care (Tai and Wang, 2001; Tai et al., 2001), we test whether activation or inhibition of PVN-VTA OT circuits/VTA-NAc DA pathways increases or suppresses paternal care using optogenetic and chemogenetic approaches. We also assess DA release in the NAc using DA sensors and *in vivo* fiber photometry. In addition, we also examined effects of activation or inhibition of PVN-NAc OT circuits on paternal behavior.

Methods and Materials

Animals

Mandarin voles were derived from individuals wild caught in Henan, China. Subjects used for the experiments were F2 generation vole reared in our laboratory at Shaanxi Normal University. Mandarin voles were housed at 22–24°C under a 12/12 h light/dark cycle with food (fresh carrots and rabbit chow) and water *ad libitum*. All procedures were conducted in accordance with the Animal Care and Use Committee of Shaanxi Normal University and approved by the Guide for the Care and Use of Laboratory Animals of China.

Stereotactic surgery and intracranial injection

Male mandarin voles (~70 d of age) were anesthetized with isoflurane and positioned in a stereotaxic apparatus got intracranial injection (RWD). Coordinates: VTA (unilateral: AP, −3.20 mm; ML, −0.45 mm; DV, −4.70 mm; bilateral: AP, −3.20 mm; ML, ±0.45 mm; DV, −4.70 mm), NAc (unilateral: AP, +1.4 mm; ML, −0.95 mm; DV, −4.25 mm; bilateral: AP, +1.4 mm; ML, ±0.95 mm; DV, −4.25 mm), and PVN (unilateral: AP, −0.7 mm; ML, −0.1 mm; DV, −5.4 mm; bilateral: AP, −0.7 mm; ML, ±0.1 mm; DV, −5.4 mm) in relation to bregma. Cholera toxin subunit B (CTB) conjugated to Alexa Fluor 488 (400 nl, BrainVTA, CTB-01) was injected into the bilateral NAc and CTB647 (400 nl, Thermo Fisher Scientific, C34778) into the bilateral VTA. retroAAV-oxytocin-Cre (400 nl, serotype titer 2/2, 6.17×10^{12} vg/ml) was delivered to the right NAc or VTA, and AAV-Ef1α-DIO-GCaMP6m (200 nl, serotype titer 2/9, 2.06×10^{12} vg/ml) was also injected into the right PVN. Subjects were injected into the VTA with virus unilaterally [AAV-Ef1α-DIO-ChR2-mCherry (200 nl, serotype titer 2/9, 3.16×10^{12} vg/ml) with AAV-TH-Cre (200 nl, serotype titer 2/9, 5.51×10^{12} vg/ml); AAV-Ef1α-DIO-mCherry (200 nl, serotype titer 2/9, 5.19×10^{12} vg/ml) with AAV-TH-Cre (200 nl, serotype titer 2/9, 5.51×10^{12} vg/ml)] or bilaterally [(AAV-Ef1α-DIO-eNpHR3.0-mCherry (200 nl, serotype titer 2/9, 2.23×10^{12} vg/ml) with AAV-TH-Cre (200 nl, serotype titer 2/9, 5.51×10^{12} vg/ml) or AAV-Ef1α-DIO-mCherry (200 nl, serotype titer 2/9, 5.19×10^{12} vg/ml) with AAV-TH-Cre (200 nl, serotype titer 2/9, 5.51×10^{12} vg/ml)]. Virus was injected unilaterally into the NAc (retroAAV-oxytocin-Cre: 400 nl, serotype titer 2/2, 6.17×10^{12} vg/ml) and the PVN (200 nl: AAV-Ef1α-DIO-mCherry, serotype titer 2/9, 5.19×10^{12} vg/ml; AAV-Ef1α-DIO-hM3Dq-mCherry, serotype titer 2/9, 2.70×10^{12} vg/ml). Virus was injected bilaterally into the NAc (retroAAV-oxytocin-Cre: 400 nl, serotype titer 2/2, 6.17×10^{12} vg/ml) and the PVN (200 nl: AAV-Ef1α-DIO-mCherry, serotype titer 2/9, 5.19×10^{12} vg/ml; AAV-Ef1α-DIO-hM4Di-mCherry, serotype titer 2/9, 5.53×10^{12} vg/ml). Virus was infused bilaterally into the VTA (retroAAV-oxytocin-Cre: 400 nl, serotype titer 2/2, 6.17×10^{12} vg/ml) and the PVN (200 nl: AAV-Ef1α-DIO-mCherry, serotype titer 2/9, 5.19×10^{12} vg/ml; AAV-Ef1α-DIO-hM3Dq-mCherry, serotype titer 2/9, 2.70×10^{12} vg/ml; AAV-Ef1α-DIO-hM4Di-mCherry, serotype titer 2/9, 5.53×10^{12} vg/ml). rAAV-CAG-dlight1.1 (400 nl, serotype titer 2/9, 5.00×10^{12} vg/ml) was infused the right NAc. All AAV were purchased from the BrainVTA Co. A 10-μl Hamilton microsyringe were used to infuse virus a rate of 100 nl/min by a microsyringe pump. The injection needle was removed 10 min after virus infusions were complete. Voles were given a recovery time of at least one week, after which they were paired with opposite sex partners to form a breeding pair.

Paternal behavior test

The paternal behavior test was performed when the pups reached postnatal day (PND)10. Pups were the father's own offspring. In the beginning of the test, fathers were placed into a novel cage (length: 32.5 cm, width: 21.5 cm, height: 16.5 cm) and habituated for 30 min. Then, a pup was placed into the cage in a corner opposite to the location of the father and father and pup interactions were recorded for 15 min. The detailed description of paternal behaviors is provided as previously described (Yuan et al., 2019). Latency to retrieve a pup: the duration from own pup exposure to hold a pup with father's mouth. Licking and grooming: licking any parts of body of own pup with father's mouth and grooming own pup's fur. Sniffing: father sniff any parts of

the body own pup. Crouching: father arched his back and strapped his own body over the pup. Inactivity: resting with no obvious movement of father's body. Licking and grooming is considered as an index of active nurturing. The other behaviors are investigatory (latency to paternal behavior and sniffing) or passive (crouching and inactivity). Mandarin vole fathers display higher levels of paternal care toward PND10 pups than toward PND1 or PND20 pups (Yuan et al., 2019).

Optogenetics and behavioral tests
Fathers (mCherry: $n = 6$, ChR2-mCherry: $n = 6$; mCherry: $n = 6$, eNpHR3.0-mCherry: $n = 8$) were implanted with optical fibers (fiber diameter = 230 μm, numerical aperture = 0.37; Shanghai Fiblaser) in the NAc (unilateral: AP, +1.4 mm; ML, +0.95 mm; DV, −4.15 mm or bilateral: AP, +1.4 mm; ML, ±1.00 mm; DV, −4.3 mm. DV: 5° angle) when the pups reached PND3. Paternal behavior tests were performed 7 d later. Optogenetic parameters were modified as in a previous study (Gunaydin et al., 2014). ChR2-injected voles received ~15 mW (473 nm, 20 Hz, 15-ms pulses) optogenetic stimulation for 15 min. For the inhibition of DAergic terminals in the NAc, eNpHR3.0-injected voles received about ~10 mw (593 nm, 5 ms, 20 Hz, 8 s on and 2 s off cycle). In the yellow light-off group, the yellow light is continuously off and behaviors were continuously recorded. In the yellow light-on group, a pulse light stimulation was given while yellow light was 8 s on and 2 s off, and behaviors were continuously recorded. A PND10 vole pup was introduced to its father and paternal behavior was compared between light on and light off epochs.

Designer receptors exclusively activated by designer drugs (DREADDs) and behavioral tests
For mCherry-hM3Dq group (PVN-VTA OT circuits: $n = 6$; PVN-NAc OT pathways: $n = 6$) or mCherry-hM4Di group (PVN-VTA OT circuits: $n = 6$; PVN-NAc OT pathways: $n = 6$), each father was first intraperitoneally injected with saline. After 30 min, the paternal behavior test was conducted for 15 min. Then, each father was intraperitoneally injected with clozapine N-oxide (CNO) immediately; 30 min later, the paternal behavior test was performed again. For mCherry group (PVN-VTA OT circuits: $n = 6$; PVN-NAc OT pathways: $n = 6$, $n = 5$), test procedure is the same as mCherry-hM3Dq group or mCherry-hM4Di group. When pups were at the age of 15 d, to detect the c-fos expression actived or inhibited by the chemogenetic stimulus after CNO injection, voles were placed in an open field for 5 min and were killed 90 min later.

Fiber photometry
For fiber photometry recording of OT neurons activity (PVN-VTA: $n = 4$–5; PVN –NAc: $n = 3$–5), an optical fiber was placed in the right PVN (−0.7 mm; ML, −0.1 mm; DV, −5.35 mm) of the father when pups were PND3. After a week, Ca^{2+} activity was recorded from OT neurons during paternal behaviors.

For recording DA signals from the genetically encoded optical DA sensor, dlight, we injected unilaterally rAAV-CAG-dlight1.1 (400 nl) into the right NAc (AP, +1.4 mm; ML, −0.95 mm; DV, −4.25 mm) as a previously described (Patriarchi et al., 2018) when the father's pups were PND1. After the virus injection, an optical fiber was immediately implanted over the right NAc (AP, +1.4 mm; ML, −0.95 mm; DV, −4.15 mm). Voles (mCherry: $n = 3$–4; Gq-mCherry: $n = 5$–7; Gi-mCherry: $n = 4$–5) were allowed to recover for two weeks before testing.

Fathers were habituated in a novel clean cage for 30 min before their own pups were introduced into the cage. Paternal

behaviors, including latency to approach a pup, retrieve, licking/ grooming, sniff and crouching were recorded as previously reported (Fang et al., 2018). Neural activity was also recorded while eating a carrot. To record OT neurons activity and DA biosensor signals, multi-channel fiber photometry system (Thinker Tech) was employed using modulated blue LED light (~50 μW) as described previously (Li et al., 2016). The emission light from a 488-nm laser was reflected by a dichroic mirror and focused by an optical objective lens (10×) coupled to an optical commutator. The light path was attached to a 0.37-NA, 230-μm optical fiber patch cord, then connected to the implanted optical fiber by a ferrule in each vole.

The recording data were analyzed in MATLAB. The $\triangle$F/F values were computed as $(F − F_0)/F_0$, where F_0 is the average of baseline fluorescence signal. For comparisons of average calcium signals, we calculated the baseline signal from −2 to 0 s and event signal from 0 to 4 s from any paternal behaviors or other non-social behaviors. For analysis of DA signals, we compared the mean values of DA signals from voles treated with saline and CNO.

Electrophysiology
Mandarin voles were anesthetized with sodium pentobarbital (50 mg/kg, i.p.). Voles were the euthanized and the brains were quickly placed in ice-cold oxygenated (95% O_2/5% CO_2) cutting solution (2.5 mM KCl, 1.25 mM NaH$_2$PO$_4$, 2 mM Na$_2$HPO$_4$, 2 mM MgSO$_4$, 213 mM sucrose, and 26 mM NaHCO$_3$). Acute brain slices containing VTA (250 μm) were sectioned with a vibratome (VT1200S, Leica). The slices were incubated in oxygenated (95% O_2/5% CO_2) artificial cerebrospinal fluid (aCSF) for at least 1 h at 34°C. Whole-cell voltage-clamp recordings were obtained from putative dopaminergic neurons detected by tyrosine hydroxylase (TH) promoter driven fluorescence using a 40× objective on a fluorescent microscope.

Immunohistochemistry
Anesthetized experimental mandarin voles were perfused transcardially with PBS (pH 7.4), followed by 4% paraformaldehyde in PBS. After perfusion, brains were postfixed for 3 d. Brains were transferred to 30% sucrose solution for ~5 d until saturated.

Coronal sections were cut on a cryostat. Sections were washed with 0.01 M PBS for 10 min. Sections were then incubated with 0.6% H_2O_2 for 20 min, and sections were rinsed three times for 5 min each (3 × 5 min) with 0.01 M PBS. Sections were then permeabilized for 20 min in 0.5% Triton X-100 and blocked with normal goat serum for 1 h at room temperature. The primary antibodies (1:7500 mouse anti-OT: Millipore, MAB5296; 1:2000 rabbit anti-TH: Abcam, ab112; 1:1500 rabbit anti-c-Fos: Abcam, ab190289) were incubated with the sections for 24 h at 4°C. The next day, the sections were washed for 3 × 5 min with 0.01 M PBS followed by incubation with the secondary antibodies (anti-rabbit goat conjugated with DyLight 488, anti-mouse goat conjugated with DyLight 488 or anti-mouse goat conjugated with Cy3) for 1 h in a 37°C water bath. Sections were then rinsed 3 × 5 min in PBS and counterstained with 4',6-diamidino-2'-phenylindole dihydrochloride (DAPI) for 10 min. Sections were washed again 3 × 5 min with 0.01 M PBS. The glass slides were fixed with antifade solution and coverslipped. Images were acquired under a Nikon microscope.

Data analysis
Parametric tests were used because all data were normally distributed based on sample Kolmogorov–Smirnov tests. Two-way
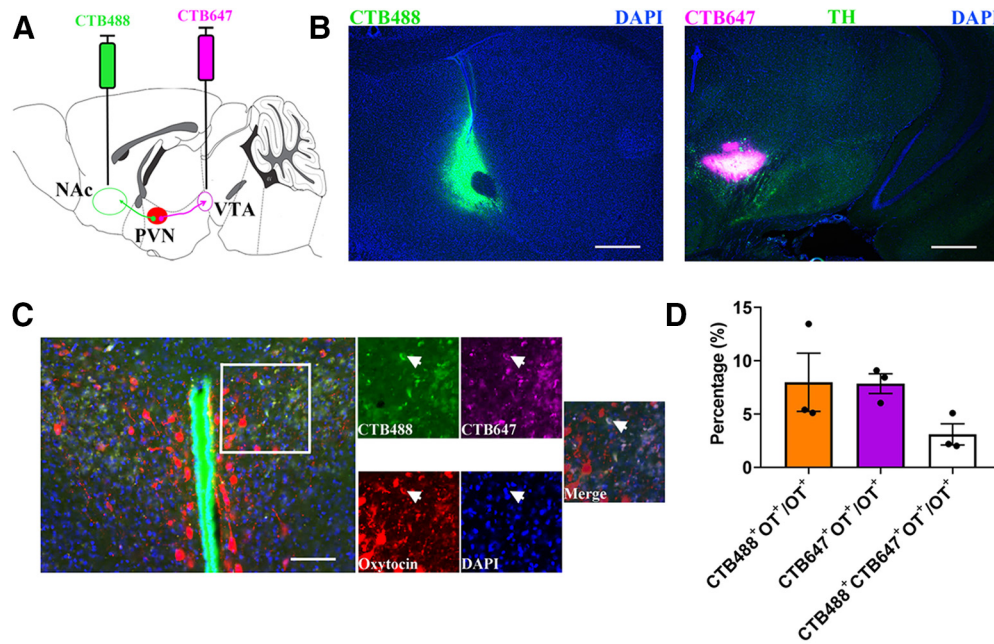
Figure 1. Anatomically distinct OT neurons project from PVN to the NAc and VTA. ***A***, Experimental schematics for determine collaterals between pairwise injected PVN OT projections. ***B***, Histology of CTB488 injection sites in the NAc (left) and CTB647 injection sites in the VTA (right). Scale bar: 500 μm. TH, tyrosine hydroxylase; DAPI, 4',6-diamidine-2'-phenylindole dihydrochloride. ***C***, An example with three-labeled PVN OT cells (red) is shown after injection of CTB-488 (green) into NAc and CTB-647 (violet) into VTA (indicated by arrowheads). Scale bar: 100 μm. ***D***, Quantification of CTB + and overlapping neurons in all PVN OT population; $n = 3$.

ANOVA for repeated-measures [chemogenetics manipulation of the PVN-VTA OT projection: treatment (mCherry/hM3Dq/hM4Di) × stimulus (saline/CNO); optogenetics: treatment (mCherry/ChR2 or mCherry/eNpHR3.0) × stimulus (light off/light on); chemogenetic manipulation of the PVN-NAc OT projection: treatment (mCherry/hM3Dq or mCherry/hM4Di) × stimulus (saline/CNO)] were used to assess overall paternal behaviors (licking/grooming, sniffing and crouching, inactivity, latency to retrieve a pup), and behavioral variables in the elevated plus maze and the open field (DREADDs experiment). Sidak multiple comparison *post hoc* tests were used to compare individual groups with significant interactions. Independent or paired t tests were used where appropriate when main effects were significant without significant interactions. For the percentages of mCherry neurons expressing Fos (PVN-NAc OT pathway) and behavioral variables in the elevated plus maze and the open field of optogenetic experiments, group comparisons were performed using independent sample t tests (two-tailed). Paired t test was used to analyze DA (saline vs CNO; baseline: −2–0 s vs event signal: 0–4 s) and Ca^{2+} signals (baseline: −2–0 s vs event signal: 0–4 s). The percentages of mCherry neurons expressing Fos (PVN-VTA OT pathway) were analyzed using a one-way ANOVA. Significance was considered as $p < 0.05$. Data are expressed as mean ± SEM SPSS 17.0 was used to analyze all data.

Results

PVN OT cells project to VTA and NAc
To confirm that PVN OT neurons project to VTA or NAc, we injected a retrograde tracer (CTB) conjugated to Alexa Fluor 647 into the VTA or CTB488 into the NAc (Fig. 1*A,B*). We found that CTB647 and/or CTB488 was colocalized with OT immunoreactivity in the PVN (Fig. 1*C*). Among all PVN OT cells, 7.86 ± 0.93% cells were labeled in CTB 647 from the VTA, 7.99 ± 2.73% neurons were labeled in CTB 488 from the NAc

and 2.49 ± 0.39% of neurons were labeled from these two brain regions ($n = 3$ animals; Fig. 1*D*). In our study, percentages of both PVN OT cells to NAc and VTA projections in the total labeled OT neurons are ~8%. The extent of overlap is much higher than the chance level = 8% × 8% = 0.64%. This suggests that a population of PVN OT neurons may bifurcate to NAc and VTA in male mandarin voles.

PVN-VTA OT neurons are activated during paternal care and carrot consumption
The activity of OT neurons in the PVN is enhanced during social interaction (Hung et al., 2017; He et al., 2019; Tang et al., 2020). To investigate whether PVN OT neurons that project to the VTA are activated during paternal care, we injected retroAAV-oxytocin-Cre into the VTA and AAV-Ef1a-DIO-GCaMP6m in the PVN (Fig. 2*A*). Immunohistochemistry revealed that 113/149 = 75.8% ($n = 2$ voles) of GCaMP6m immunoreactive neurons were OT-positive cells (Fig. 2*B,C*). We implanted optical fibers into the PVN and measured changes of Ca^{2+} signals using fiber photometry (Fig. 2*D*). In the experiment, fathers were allowed to freely interact with his pups in a novel cage. Fathers displayed increased intracellular Ca^{2+} concentrations in putative VTA projecting PVN OT neurons during approaching ($p = 0.017$; Fig. 2*E, E'*), first sniffing ($p < 0.001$; Fig. 2*F,F'*), retrieving ($p = 0.044$; Fig. 2*G,G'*), and licking and grooming ($p = 0.029$; Fig. 2*H,H'*) their pups. As the father quietly crouched over the pups ($p = 0.291$; Fig. 2*I,I'*), selfgroomed ($p = 0.310$; Fig. 2*J,J'*), and sniffed an object ($p = 0.690$; Fig. 2*K,K'*), PVN–VTA OT neuronal activity was not changed. Interestingly, PVN to VTA OT projections were activated on approaching/eating carrot ($p = 0.028$; Fig. 2*L,L'*).

PVN to VTA OT projection promote active paternal nurturing
OT neurons in the PVN project to the VTA, and OT release in the VTA enhances the activity of a reward-specific population of
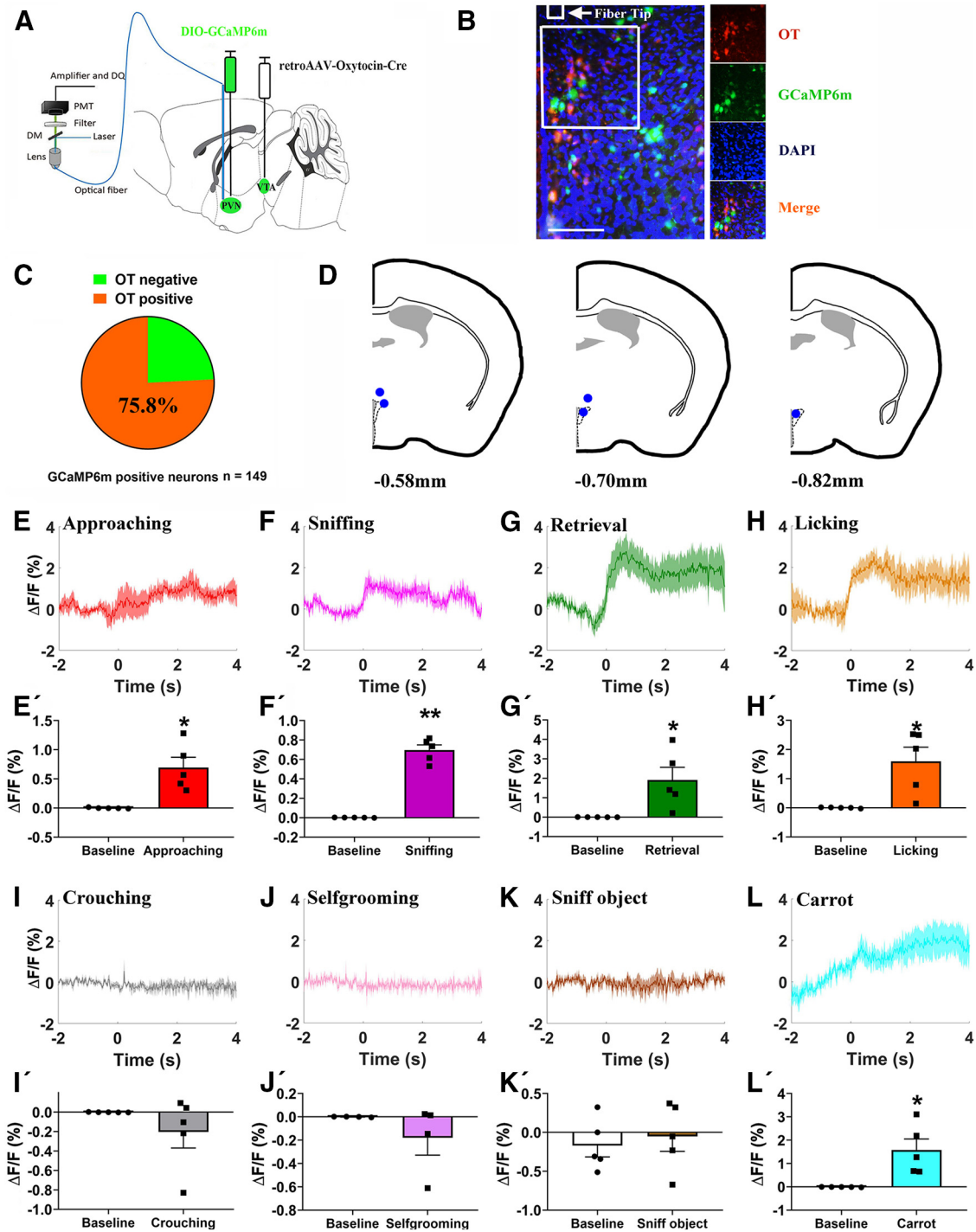
Figure 2. Paternal behaviors and carrot consumption evoked activation of VTA projecting PVN OT neuron. ***A***, Schematic of viral injection and optical fiber implantation above the PVN. ***B***, Co-localization of immunoreactive GCaMP6m (green), OT (red), and DAPI (blue) and the optical fiber location in the PVN. Scale bar: 100 μm. ***C***, Statistical chart showed that GCaMP6m was relatively restricted to OT-positive neurons ($n = 2$). ***D***, Schematic diagrams showing the target of fiber tip placements in the PVN. ***E–L***, Average $\triangle$F/F during various paternal behaviors: (***E***) approaching, (***F***) sniffing, (***G***) retrieval, (***H***) grooming, (***I***) crouching, (***J***) selfgrooming, (***K***) sniff object, and (***L***) approaching/eating carrot. ***E′–L′***, Comparison of average calcium signal for −2–0 and 0–4 s after various paternal behaviors: (***E′***) approaching ($t_{(4)} = −3.932$, $p = 0.017$), (***F′***) first sniffing ($t_{(4)} = −13.084$, $p < 0.001$), (***G′***) retrieval ($t_{(4)} = −2.905$, $p = 0.044$), (***H′***) grooming ($t_{(4)} = −3.332$, $p = 0.0290$), (***I′***) crouching ($t_{(4)} = 1.216$, $p = 0.291$), (***J′***) selfgrooming ($t_{(3)} = 1.220$, $p = 0.310$), (***K′***) sniff object ($t_{(4)} = −0.429$, $p = 0.690$), and (***L′***) approaching/eating carrot ($t_{(4)} = −3.358$, $p = 0.028$); $n = 4–5$. Paired t test; *$p < 0.05$, **$p < 0.01$. Data are mean $\pm$ SEM.

VTA DA neurons in mice (Hung et al., 2017). We hypothesized that activating PVN to VTA OT inputs would enhance paternal behaviors. To test this, we bilaterally injected retroAAV-oxytocin-Cre into the VTA to express *Cre* in OT neurons projecting to the VTA, and Cre-dependent hM3Dq or hM4Di into the PVN of the experimental group to chemogenetically activate or inhibit OT neuron activity using CNO (Fig. 3A). Controls were injected AAV-EF1α-DIO-mCherry and all animals received saline or CNO. Here, 227/242 = 93.8% of hM3Dq-mCherry+ neurons or 214/225 = 95.1% of hM4Di-mCherry+ neurons were OT immunoreactive ($n = 2$ voles; Fig. 3B,C).
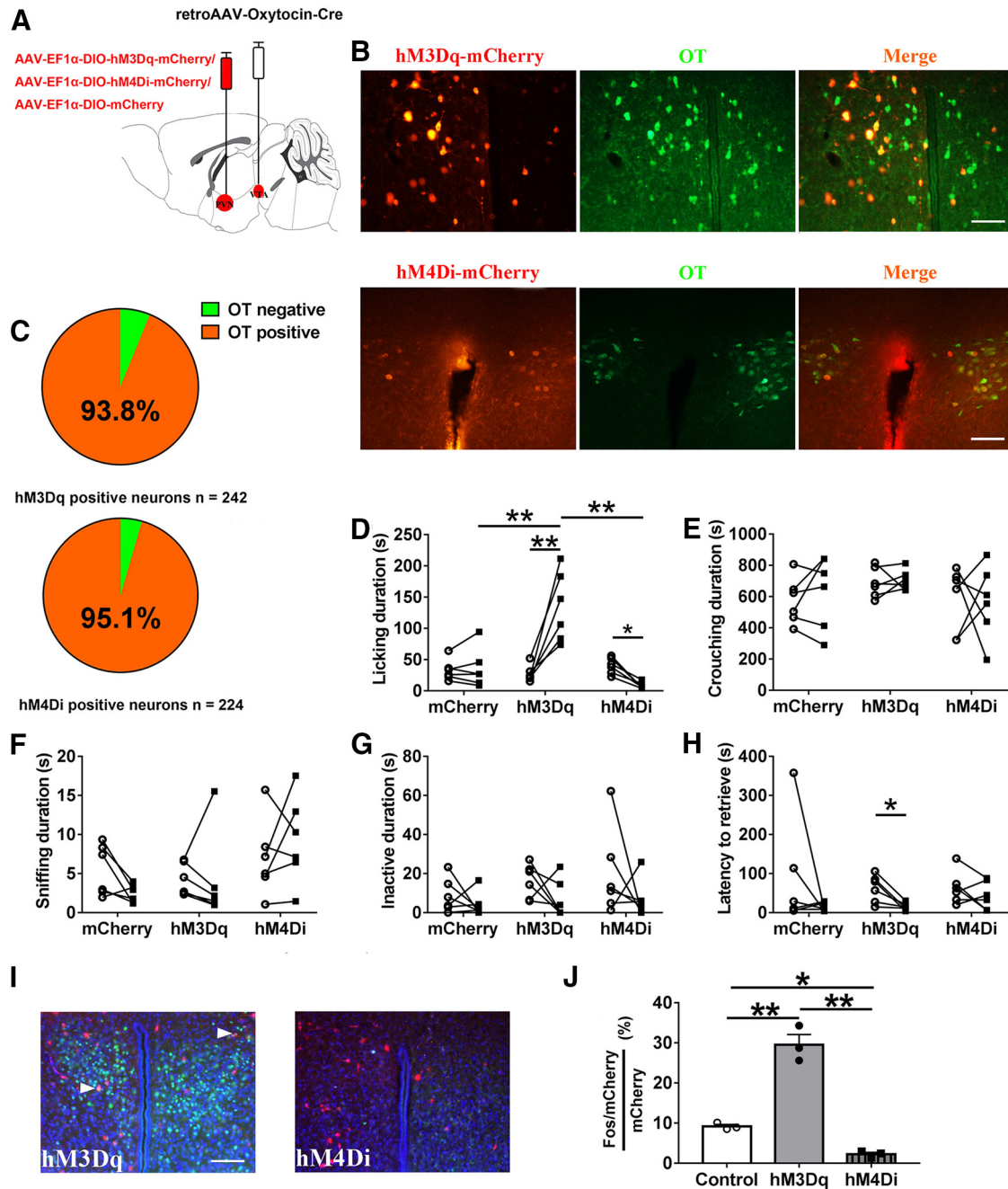
Figure 3. Influences of chemogenetic activation/inhibition of the PVN to VTA OT circuit on paternal behaviors. **A**, Schematic of AAV injection. **B**, Confocal image depicting OT immunostaining (green), hM3Dq-mCherry/hM4Di-mCherry immunostaining (red), and DAPI (blue) in the PVN. Scale bar: 100 μm. **C**, Statistical chart showed that hM3Dq-mCherry ($n = 2$) or hM4Di-mCherry neurons ($n = 2$) were relatively restricted to OT-positive cells. **D–H**, Effects of chemogenetic activation (hM3Dq) or inhibition (hM4Di) of PVN OT neurons projecting to VTA on the duration of (**D**) licking/grooming (interaction: $F_{(2,15)} = 27.447$, $p < 0.001$, post hoc test: mCherry saline vs CNO, $p = 0.850$; hM3Dq saline vs CNO, $p < 0.001$; hM4Di saline vs CNO, $p = 0.035$; saline mCherry vs hM3Dq, $p = 0.866$; saline mCherry vs hM4Di, $p = 0.801$; saline hM3Dq vs hM4Di, $p = 0.370$; CNO mCherry vs hM3Dq, $p = 0.001$; CNO mCherry vs hM4Di, $p = 0.522$; CNO hM3Dq vs hM4Di, $p < 0.001$), (**E**) crouching (interaction: $F_{(2,15)} = 0.152$, $p = 0.861$; treatment: $F_{(1,15)} = 0.114$, $p = 0.740$; group: $F_{(2,15)} = 1.480$, $p = 0.259$), (**F**) sniffing pup (interaction: $F_{(1,15)} = 1.982$, $p = 0.172$; treatment: $F_{(1,15)} = 0.077$, $p = 0.785$; group: $F_{(2,15)} = 2.832$, $p = 0.091$), (**G**) inactivity (interaction: $F_{(2,15)} = 0.276$, $p = 0.763$; treatment: $F_{(1,15)} = 3.454$, $p = 0.083$; group: $F_{(2,15)} = 1.836$, $p = 0.194$), and (**H**) the latency to retrieve a pup (interaction: $F_{(2,15)} = 0.548$, $p = 0.590$; treatment: $F_{(1,15)} = 4.969$, $p = 0.042$, hM3Dq saline vs CNO, paired t test: $t_{(5)} = 3.390$, $p = 0.019$; group: $F_{(2,15)} = 0.193$, $p = 0.827$). Sample sizes are $n = 6$ for each group. Data were analyzed by two-way ANOVA with repeated measures; *$p < 0.05$, **$p < 0.01$. Data are mean $\pm$ SEM. **I**, Representative images of the PVN illustrating c-Fos in neurons expressing hM3Dq-mCherry. Scale bar: 100 μm. **J**, Percentage of mCherry+ neurons that were also Fos+ in the PVN after CNO injection ($n = 3$; $F_{(2,6)} = 87.264$, $p < 0.001$, post hoc test: control vs hM3Dq, $p < 0.001$; control vs hM4Di, $p = 0.041$; hM3Dq vs hM4Di, $p < 0.001$). One-way ANOVA; *$p < 0.05$, **$p < 0.01$. Data are mean $\pm$ SEM.

hM3Dq-mCherry (activation) fathers engaged in more licking/ grooming after CNO injection compared with saline injection ($p < 0.001$), while hM4Di-mCherry (inhibition) fathers engaged in less licking/grooming after CNO injection compared with saline injection ($p = 0.0350$), CNO treatments did not affect total

duration of licking/grooming in mCherry (control) fathers (Fig. 3D). hM3Dq-mCherry fathers engaged in significantly more licking/grooming than hM4Di-mCherry fathers ($p < 0.001$) and mCherry fathers ($p = 0.001$) after CNO injection (Fig. 3D). Chemogenetic activation/inhibition of PVN to VTA OT inputs
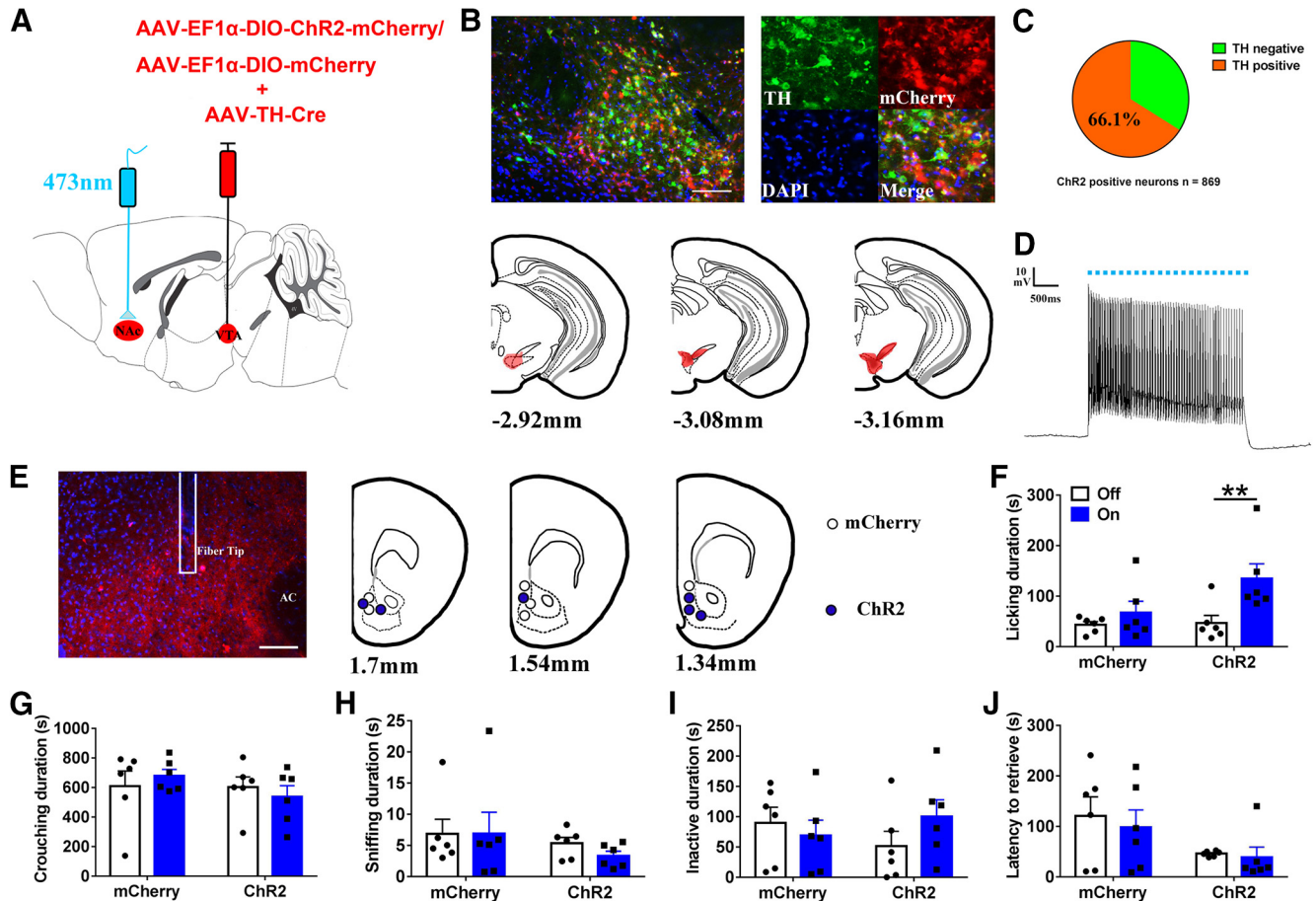
Figure 4. Optogenetic activation of VTA-originating DA terminals in NAc increased licking and grooming of fathers for own pups. **A**, Schematic of viral strategy and optical fiber implantation above the NAc. **B**, Overlap of TH immunoreactivity (green), ChR2 expression (red), and DAPI (blue) in the VTA (up); schematic representations of the viral injection spread in the VTA (down). Scale bar: 100 μm. **C**, Statistical chart showed that ChR2-mCherry was relatively restricted to TH-positive cells ($n = 2$). **D**, Optical stimulation evoke action potentials of a ChR2-expressing neuron in the VTA. **E**, Confocal image showing axonal mCherry signal and the optical fiber track in the NAc. Scale bar: 100 μm. AC: anterior commissure. **F–J**, Effect of activating the VTA to NAc DA pathways on the total of time spent on (**F**) licking/grooming (interaction: $F_{(1,10)} = 5.459$, $p = 0.042$, post hoc test: ChR2 off vs on, $p = 0.001$; mCherry off vs on, $p = 0.250$; light off ChR2 vs mCherry, $p = 0.839$; light on ChR2 vs mCherry, $p = 0.098$), (**G**) crouching (interaction: $F_{(1,10)} = 0.753$, $p = 0.406$; treatment: $F_{(1,10)} = 0.001$, $p = 0.980$; group: $F_{(1,10)} = 1.047$, $p = 0.330$), (**H**) sniffing (interaction: $F_{(1,10)} = 0.216$, $p = 0.652$); treatment: $F_{(1,10)} = 0.195$, $p = 0.668$; group: $F_{(1,10)} = 1.487$, $p = 0.251$), (**I**) inactivity (interaction: $F_{(1,10)} = 2.766$, $p = 0.127$; treatment: $F_{(1,10)} = 0.439$, $p = 0.522$; group: $F_{(1,10)} = 0.014$, $p = 0.907$), and (**J**) the latency to retrieve a pup (interaction: $F_{(1,10)} = 0.008$, $p = 0.929$; treatment: $F_{(1,10)} = 0.116$, $p = 0.741$; group: $F_{(1,10)} = 2.567$, $p = 0.140$). mCherry ($n = 6$), ChR2-mCherry ($n = 6$). Two-way ANOVA with repeated measures; **$p < 0.01$. Error bars indicate SEM.

did not affect crouching (Fig. 3E), sniffing pups (Fig. 3F), and inactivity (Fig. 3G). Systemic CNO decreased the latency of hM3Dq-mCherry fathers to retrieve a pup compared with saline treatment ($p = 0.019$), but did not affect the latency to retrieve a pup in hM4Di-mCherry fathers (Fig. 3H). After CNO administration, the percentage of hM3Dq cells expressing c-Fos was significantly increased compared with mCherry control cells ($p < 0.001$). Conversely, the percentage of hM4Di cells expressing Fos was significantly reduced compared with control mCherry cells ($p = 0.041$). Finally, the percentage of hM3Dq cells that were Fos+ was significantly increased compared with hM4Di cells ($p < 0.001$). These results confirmed and validated that chemogenetic activation and inhibition of OT neurons projecting to the VTA was achieved (Fig. 3I,J).

Dopaminergic VTA projections to the NAc promote active paternal nurturing
Optogenetic activation of VTA to NAc DA pathway promoted pup licking/grooming
In order to optogenetically activate VTA DA neuron (expressing *Th*) terminals in the NAc, we injected AAV-TH-Cre plus AAV-

EF1α-DIO-ChR2-mCherry into the VTA (Fig. 4A). Immunohistochemical analysis revealed that the majority of neurons expressing ChR2 (mCherry+) were also immunopositive for TH (574/869 = 66.1%, from two voles; Fig. 4B,C). Photostimulation robustly evoked depolarized action potentials in ChR2- mCherry-expressing neurons in the VTA (Fig. 4D). Optical fibers were implanted in the NAc (Fig. 4E).

Optogenetic stimulation of VTA terminals in the NAc increased the time spent actively nurturing (e.g., licking and grooming; $p = 0.001$; Fig. 4F) but had no effect on the duration of crouching (Fig. 4G), sniffing pups (Fig. 4H), or inactivity (Fig. 4I) or the latency to retrieve a pup (Fig. 4J).

Optogenetic inhibition of VTA to NAc DA pathways reduces active paternal nurturing
In order to inhibit terminals of VTA DA neurons in the NAc, we expressed a halorhodopsin (NpHR3.0) in VTA DA neurons by injecting AAV-TH-cre and a Cre-dependent AAV encoding NpHR3.0 fused to mCherry into the VTA (Fig. 5A). Histologic analysis revealed that NpHR3.0-mCherry was largely confined in the TH neurons (621/906 = 68.5%, $n = 2$ animals; Fig. 5B,C). Optical stimulation efficiently inhibited firing of eNpHR3.0-
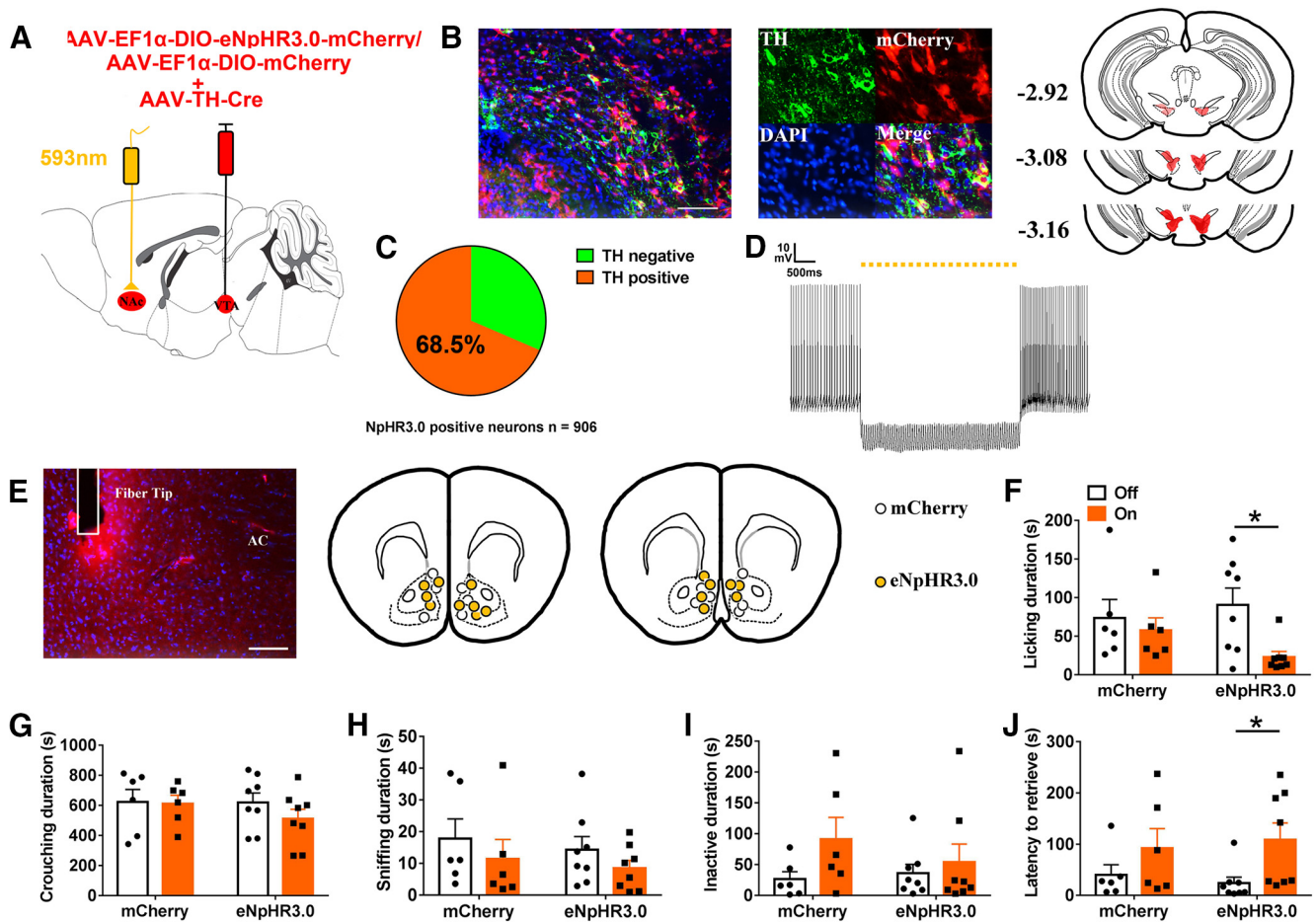
Figure 5. Optogenetic inhibition of VTA to NAc DA pathways in NAc decreased paternal behaviors. **A**, Schematic of viral injection and optical fiber implantation above the NAc. **B**, Co-localization of TH immunoreactivity (green), eNpHR3.0 expression (red), and DAPI (blue) in the VTA (left); schematic representations of the viral injection spread in the VTA (right). Scale bar: 100 μm. **C**, Statistical chart showed that eNpHR3.0-mCherry was relatively restricted to TH-positive cells (n = 2). **D**, Trace showing the yellow light stimulation inhibits firing of a eNpHR3.0-expressing neuron in the VTA. **E**, Confocal images showing axonal mCherry signal and the optical fiber track in the NAc. Scale bar: 100 μm. AC: anterior commissure. **F–J**, Effect of inhibition of VTA to NAc DA pathways on the total of time spent (**F**) licking/grooming the pup (interaction: $F_{(1,12)} = 2.009$, $p = 0.182$; treatment: $F_{(1,12)} = 5.271$, $p = 0.041$, eNpHR3.0 off vs on, paired t test: $t_{(7)} = 3.333$, $p = 0.013$; group: $F_{(1,12)} = 0.223$, $p = 0.645$), (**G**) crouching (interaction: $F_{(1,12)} = 0.599$, $p = 0.454$; treatment: $F_{(1,12)} = 0.878$, $p = 0.367$; group: $F_{(1,12)} = 0.525$, $p = 0.482$), (**H**) sniffing the pup (interaction: $F_{(1,12)} = 0.009$, $p = 0.925$; treatment: $F_{(1,12)} = 4.499$, $p = 0.055$; group: $F_{(1,12)} = 0.293$, $p = 0.598$), (**I**) inactivity (interaction: $F_{(1,10)} = 0.868$, $p = 0.370$; treatment: $F_{(1,10)} = 2.727$, $p = 0.125$; group: $F_{(1,12)} = 0.302$, $p = 0.593$), and (**J**) the latency to retrieve a pup (interaction: $F_{(1,12)} = 0.408$, $p = 0.535$; treatment: $F_{(1,12)} = 7.205$, $p = 0.020$, eNpHR3.0 off vs on, paired t test: $t_{(7)} = -2.488$, $p = 0.042$; group: $F_{(1,12)} < 0.01$, $p = 0.995$; **I**). mCherry (n = 6), eNpHR3.0-mCherry (n = 8). Two-way ANOVA with repeated measures; *$p < 0.05$. Error bars indicate SEM.

expressing neurons in the VTA (Fig. 5D). We implanted the optical fiber into the NAc (Fig. 5E).

Optogenetic inhibition of DAergic VTA terminals in NAc reduced active nurturing behaviors, i.e., duration of licking/grooming ($p = 0.013$; Fig. 5F), and increased the latency to retrieve a pup ($p = 0.042$; Fig. 5J). Optogenetic inhibition did not influence investigatory or passive behaviors such as crouching (Fig. 5G), sniffing pups (Fig. 5H), or inactivity (Fig. 5I).

PVN OT neurons projecting to VTA enhance DA release in the NAc during active paternal nurturing

To investigate whether chemogenetic activation or inhibition of the PVN to VTA OT circuit affects DA release in the NAc, we examined DA release in the NAc during paternal behaviors using a genetically encoded DA sensor, dLight1.1 (Patriarchi et al., 2018), with optical fibers implanted above the NAc (Fig. 6A,B).

The DA signal changes were recorded by in vivo fiber photometry while a father interacted with his own pup and registered to approach, sniffing, retrieval, licking/grooming and crouching or while sniff object, selfgrooming, and approaching/eating a carrot. In control and hM3Dq group, DA signals

increased significantly on approaching, sniffing pups first time, retrieval, licking and grooming pups, and approaching/eating carrot after saline or CNO injection (Fig. 6C9,C10,D9,D10). As the fathers quietly crouched over their pups, selfgrooming, or sniffing object, DA signals did not change in fathers regardless of treatment (Fig. 6C9,C10,D9,D10). In the hM4Di group, release of DA is similar with control and hM3Dq group after saline treatment (Fig. 6E9), DA signals also increased in the NAc as they were approaching, retrieving or sniffing pups after CNO injection, but not in licking own pups, approaching/eating carrot, crouching, selfgrooming, and sniffing object (Fig. 6E10).

Compared with saline-injected controls (Fig. 6C1–C8'), chemogenetic activation of PVN to VTA OT circuits did not affect DA sensor signal on approaching (Fig. 6D1,D1'), first sniff own pups (Fig. 6D2,D2'), retrieval (Fig. 6D3,D3'), licking own pups (Fig. 6D4,D4'), crouching (Fig. 6D5,D5'), selfgrooming (Fig. 6D6,D6'), sniff object (Fig. 6D7,D7'), or approaching/eating carrot (Fig. 6D8,D8').

In contrast, inhibition of the PVN to VTA OT circuit with hM4Di plus CNO significantly reduced DA signals during licking and grooming ($p = 0.012$; Fig. 6E4,E4') and approach/eating
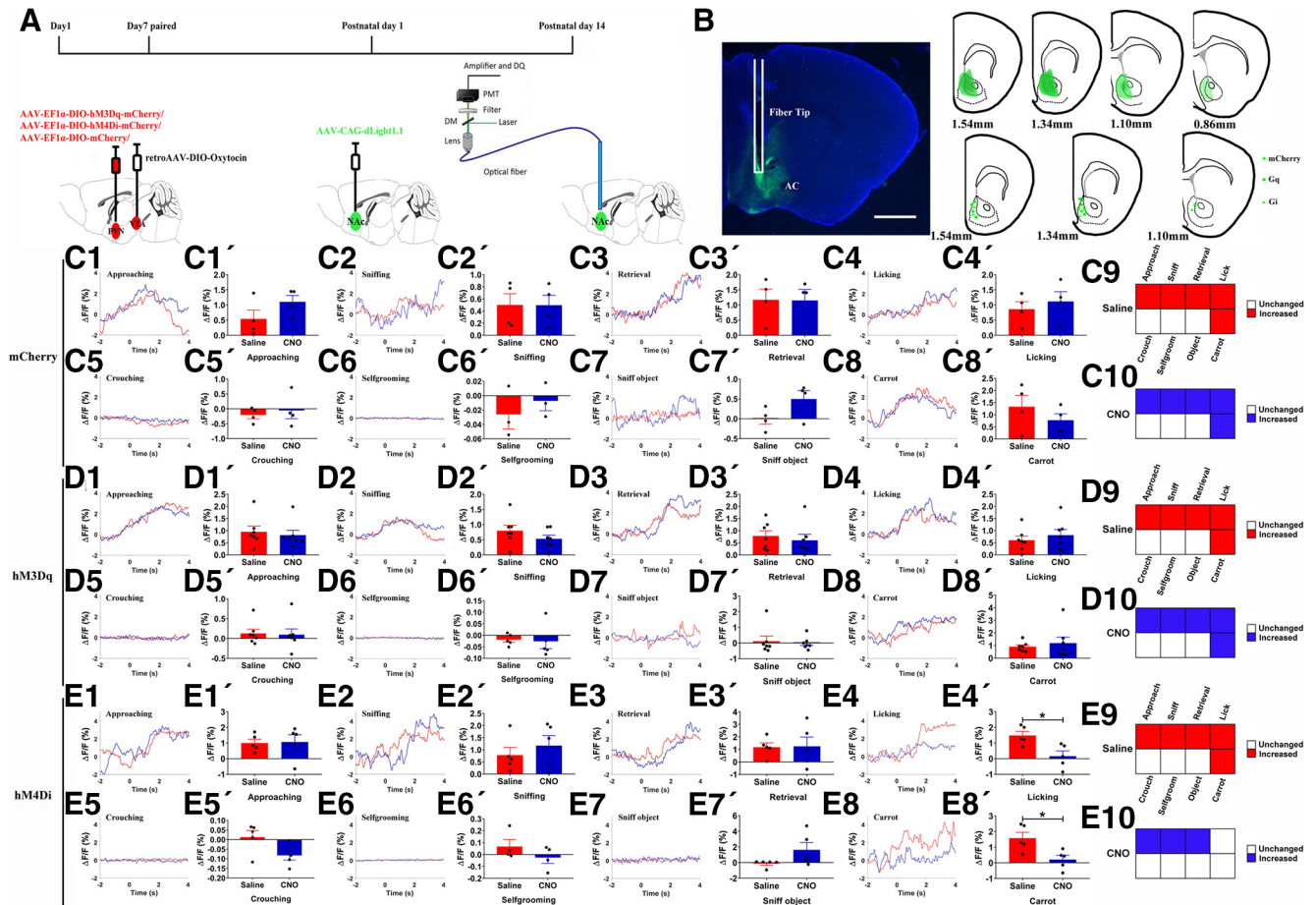
Figure 6. Chemogenetic activation/inhibition of PVN-NAc projections influenced DA release in the NAc simultaneously on paternal behaviors. *A*, Experimental design. *B*, dLight1.1 expression and fiber tips location in the NAc (left), schematic representations of the viral injection spread in the NAc (right). Scale bar: 1 mm. *C1–E8*, Representative traces showing DA signal changes aligned to onsets of various paternal behaviors (*C1–C5, D1–D5, E1–E5*), selfgrooming (*C6, D6, E6*), sniff object (*C7, D7, E7*), or approach/eating carrot (*C8, D8, E8*). 1 = approach, 2 = first sniff own pups, 3 = retrieval, 4 = licking, 5 = crouching, 6 = selfgrooming, 7 = sniff object, 8 = carrot. *C1′–E8′*, Mean △F/F during approaching (mCherry: $t_{(3)} = -1.548$, $p = 0.219$; Gq: $t_{(6)} = 0.430$, $p = 0.682$; Gi: $t_{(4)} = -0.099$, $p = 0.926$; *C1′, D1′, E1′*), first sniff own pups (mCherry: $t_{(3)} = 0.012$, $p = 0.991$; Gq: $t_{(6)} = 1.096$, $p = 0.315$; Gi: $t_{(4)} = -0.593$, $p = 0.585$; *C2′, D2′, E2′*), retrieval (mCherry: $t_{(3)} = 0.095$, $p = 0.931$; Gq: $t_{(6)} = 0.861$, $p = 0.422$; Gi: $t_{(4)} = -0.076$, $p = 0.943$; *C3′, D3′, E3′*), licking (mCherry: $t_{(3)} = -1.122$, $p = 0.344$; Gq: $t_{(6)} = -1.179$, $p = 0.283$; Gi: $t_{(4)} = 4.341$, $p = 0.012$; *C4′, D4′, E4′*), crouching (mCherry: $t_{(3)} = -0.702$, $p = 0.533$; Gq: $t_{(6)} = 0.155$, $p = 0.882$; Gi: $t_{(4)} = 2.619$, $p = 0.059$; *C5′, D5′, E5′*), selfgrooming (mCherry: $t_{(2)} = -0.661$, $p = 0.577$; Gq: $t_{(4)} = 0.234$, $p = 0.826$; Gi: $t_{(3)} = 1.758$, $p = 1.777$; *C6′, D6′, E6′*), sniff object (mCherry: $t_{(3)} = -1774$, $p = 0.174$; Gq: $t_{(6)} = 0.353$, $p = 0.736$; Gi: $t_{(4)} = -1.946$, $p = 0.124$; *C7′, D7′, E7′*), or approach/eating carrot (mCherry: $t_{(3)} = 1.814$, $p = 0.167$; Gq: $t_{(6)} = -0.572$, $p = 0.588$; Gi: $t_{(4)} = 2.841$, $p = 0.047$; *C8′, D8′, E8′*) shown in all fathers. *C9, C10, D9, D10, E9, E10*, Tuning matrix for DA release (baseline vs signals) in mCherry (*C9, C10*), Gq-mCherry (*D9, D10*), and Gi-mCherry (*E9, E10*) groups, these DA changes are relative to the. mCherry: $n = 3$–4; Gq-mCherry: $n = 5$–7; Gi-mCherry: $n = 4$–5. Paired t test; *$p < 0.05$. Error bars indicate SEM.

carrot ($p = 0.047$; Fig. 6E8,E8′), whereas it did not alter DA signals on approaching (Fig. 6E1,E1′), first sniffing pups (Fig. 6E2, E2′), retrieval (Fig. 6E3,E3′), crouching over (Fig. 6E5,E5′) their pups, selfgrooming (Fig. 6E6,E6′), sniff object (Fig. 6E7,E7′).

PVN OT neurons projecting to NAc are activated during paternal care

Social reward in mice is mediated in part by PVN OT projections to the NAc (Dölen et al., 2013). To test whether PVN OT projections to NAc are activated during paternal care, we injected retroAAV-oxytocin-Cre into the NAc and AAV-Ef1a-DIO-GCaMP6m in the PVN (Fig. 7A), and implanted optical fibers into the PVN (Fig. 7D). The majority of neurons expressing GCaMP6m co-expressed OT (184/227 = 81.1%, $n = 2$ voles; Fig. 7B,C). We recorded GCaMP6m fluorescence while the father interacted with his pup. We observed Ca^{2+} signals from five voles. One vole did not retrieve his pups, but the vole was not excluded from subsequent analysis. A significant intracellular Ca^{2+} increase was observed while fathers were approaching

($p = 0.017$; Fig. 7E,E′), sniffing ($p = 0.031$; Fig. 7F,F′), retrieving ($p = 0.040$; Fig. 7G,G′), and licking and grooming ($p = 0.005$; Fig. 7H,H′) their own pups. However, the PVN to NAc OT neurons were not activated on crouching ($p = 0.422$; Fig. 7I,I′), selfgrooming ($p = 0.992$; Fig. 7J,J′), sniffing object ($p = 0.168$; Fig. 7K,K′), and approaching/eating carrot ($p = 0.987$; Fig. 7L,L′).

PVN OT neurons projecting to NAc promote active paternal nurturing

Chemogenetic activation of PVN to NAc OT inputs enhances active paternal nurturing
To examine whether this circuit plays a role in paternal behaviors, we expressed hM3Dq in the PVN and injected retroAAV-oxytocin-Cre into the NAc (Fig. 8A). Histologic analysis revealed that hM3Dq-mCherry was largely confined in the OT cells (193/207 = 93.2%, from two voles; Fig. 8B,C).

hM3Dq-mCherry (activation) fathers engaged in more licking after CNO injection compared with saline injection ($p = 0.006$; Fig. 8D). Crouching (Fig. 8E), sniffing (Fig. 8F), and inactivity
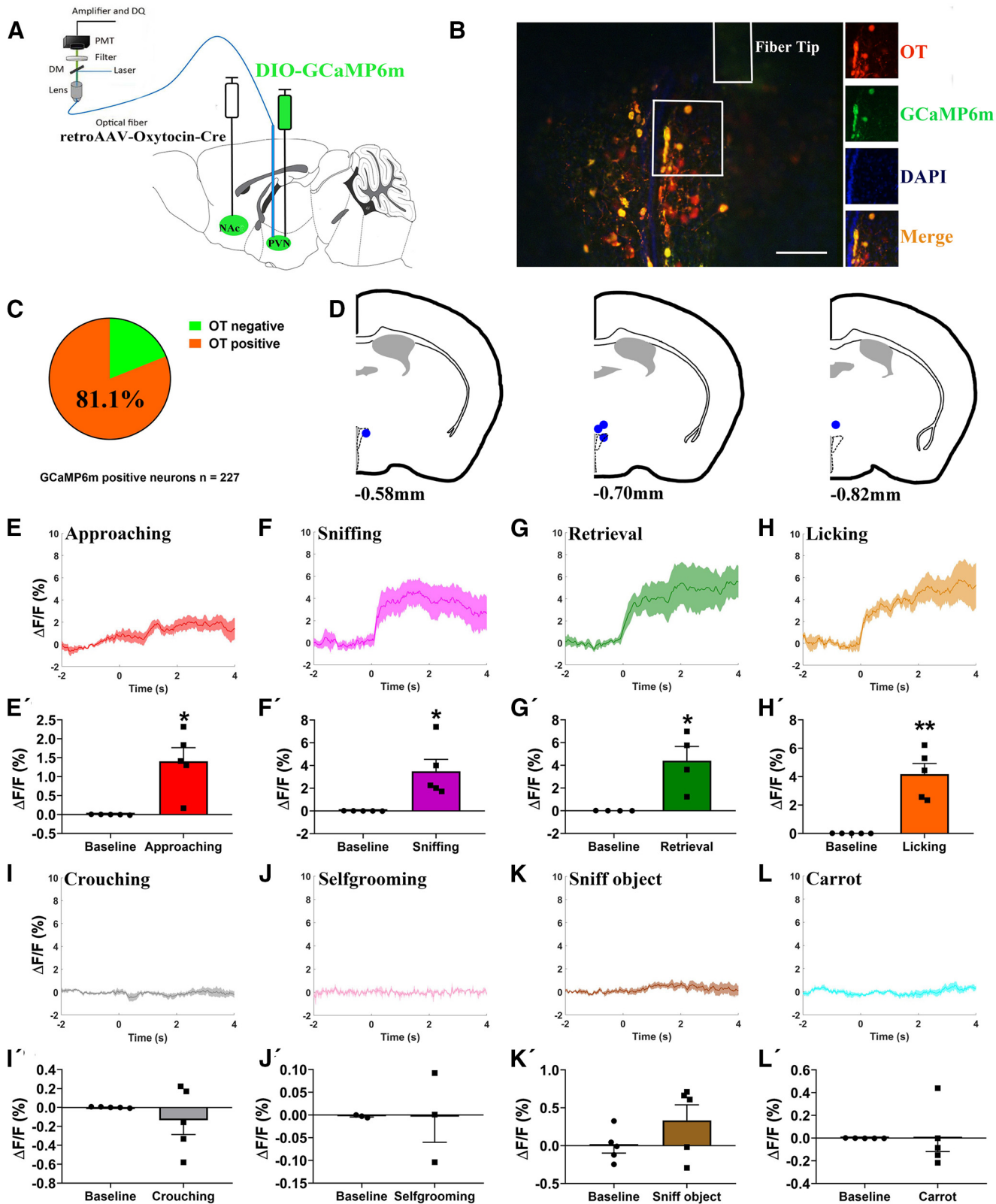
Figure 7. In *vivo* recording of PVN –NAc OT neurons on paternal behaviors. *A*, Schematic of viral injection and optical fiber implantation above the PVN. *B*, Co-localization of immunoreactive GCaMP6m (green), OT (red), and DAPI (blue) and the optical fiber location in the PVN. Scale bar: 100 μm. *C*, Statistical chart showed that GCaMP6m was relatively restricted to OT-positive neurons ($n = 2$). *D*, Schematic diagrams showing the target of fiber tip placements in the PVN. *E–L*, Average $\triangle$F/F during various paternal behaviors: (*E*) approaching, (*F*) first sniffing pups, (*G*) retrieval, (*H*) licking, (*I*) crouching, (*J*) selfgrooming, (*K*) sniff object, and (*L*) approach/eating carrot. *E′–L′*, Comparison of average calcium signal for 2 s before and 4 s after various paternal behaviors: (*E′*) approaching ($t_{(4)} = -3.921$, $p = 0.017$), (*F′*) first sniffing pups ($t_{(4)} = -3.269$, $p = 0.031$), (*G′*) retrieval ($t_{(3)} = -3.486$, $p = 0.040$), (*H′*) licking ($t_{(4)} = -5.489$, $p = 0.005$), (*I′*) crouching ($t_{(4)} = 0.893$, $p = 0.422$), (*J′*) selfgrooming ($t_{(2)} = 0.012$, $p = 0.992$), (*K′*) sniffing object ($t_{(4)} = -1.680$, $p = 0.168$), and (*L′*) approach/eating carrot ($t_{(4)} = 0.017$, $p = 0.987$); $n = 3$–5. Paired t test; *$p < 0.05$, **$p < 0.01$. Data are mean ± SEM.
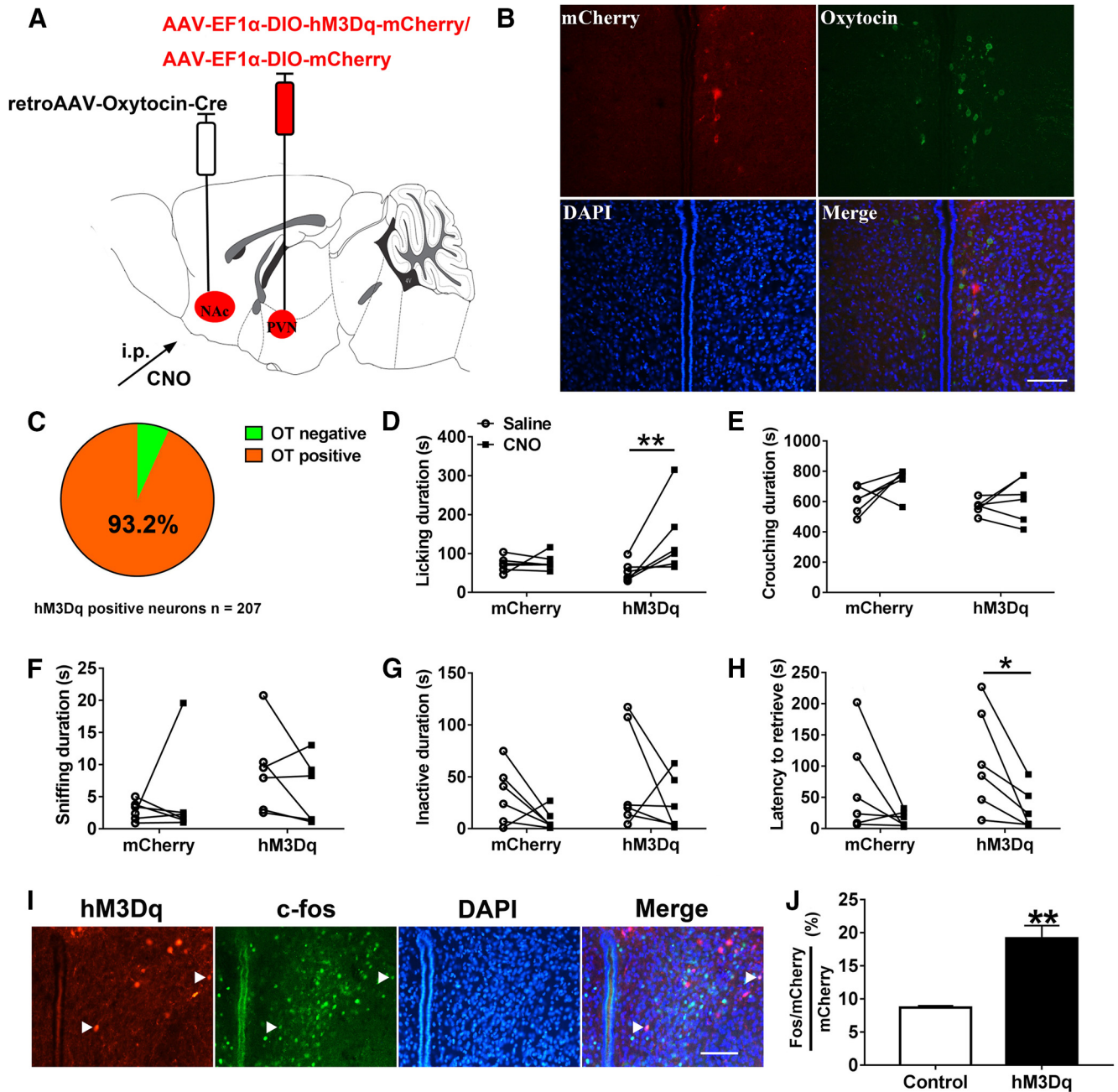
Figure 8. Chemogenetic activation of the PVN to NAc OT circuit promoted paternal behaviors. **A**, Viral strategy. **B**, Co-localization of hM3Dq expression (red), OT immunoreactivity (green), and DAPI (blue) in the PVN. Scale bar: 100 μm. **C**, Statistical chart showed that hM3Dq-mCherry was relatively restricted to OT-positive cells ($n = 2$). **D–H**, Effect of activation of PVN to NAc OT pathways on the duration of (**D**) Licking/grooming (interaction: $F_{(1,10)} = 5.103$, $p = 0.047$, *post hoc* test: hM3Dq saline vs CNO, $p = 0.006$; mCherry saline vs CNO, $p = 0.820$; saline mCherry vs hM3Dq, $p = 0.172$; CNO mCherry vs hM3Dq, $p = 0.156$), (**E**) crouching over pups (interaction: $F_{(1,10)} = 1.016$, $p = 0.337$; treatment: $F_{(1,10)} = 4.767$, $p = 0.054$; group: $F_{(1,10)} = 4.452$, $p = 0.061$), (**F**) sniffing pups (interaction: $F_{(1,10)} = 1.735$, $p = 0.217$; treatment: $F_{(1,10)} = 0.129$, $p = 0.727$; group: $F_{(1,10)} = 1.994$, $p = 0.193$), (**G**) inactivity (interaction: $F_{(1,10)} = 0$, $p = 1$; treatment: $F_{(1,10)} = 3.295$, $p = 0.100$; group: $F_{(1,10)} = 1.346$, $p = 0.273$), and (**H**) the latency to retrieve a pup (interaction: $F_{(1,10)} = 0.443$, $p = 0.521$; treatment: $F_{(1,10)} = 10.905$, $p < 0.01$, hM3Dq saline vs CNO paired t test: $t_{(5)} = 3.003$, $p = 0.030$; group: $F_{(1,10)} = 1.007$, $p = 0.324$). mCherry ($n = 6$), hM3Dq-mCherry ($n = 6$). Two-way ANOVA with repeated measures; *$p < 0.05$, **$p < 0.01$. **I**, Representative images of the PVN illustrating c-Fos in neurons expressing hM3Dq-mCherry. Scale bar: 100 μm. **J**, Percentage of mCherry neurons in the PVN that are Fos+ after CNO administration ($t_{(4)} = -5.400$, $p = 0.006$; $n = 3$). Independent t test; **$p < 0.01$. Data are mean $\pm$ SEM.

(Fig. 8G) were not affected significantly by chemogenetic activation of PVN to NAc OT circuit. After CNO injection, chemogenetic activation of PVN to NAc OT inputs reduced the latency to retrieve a pup ($p = 0.030$; Fig. 8H). After CNO injection, the percentages of mCherry neurons co-expressing c-fos were significantly higher in hM3Dq voles compared with control voles ($p = 0.006$; Fig. 8I,J) indicating that chemogenetic activation of PVN to NAc OT inputs was valid.

Chemogenetic inhibition of the PVN to NAc OT circuit suppresses active paternal nurturing

We next sought to determine whether inhibition of the PVN to NAc OT pathway decreases paternal behaviors. We injected AAV-Ef1α-DIO-hM4Di-mCherry into the PVN and retrograde AAV-oxytocin-Cre into the NAc (Fig. 9A). The majority of hM4Di-mCherry cells were confined in the OT neurons (304/396 = 76.8%, from two voles; Fig. 9B,C).
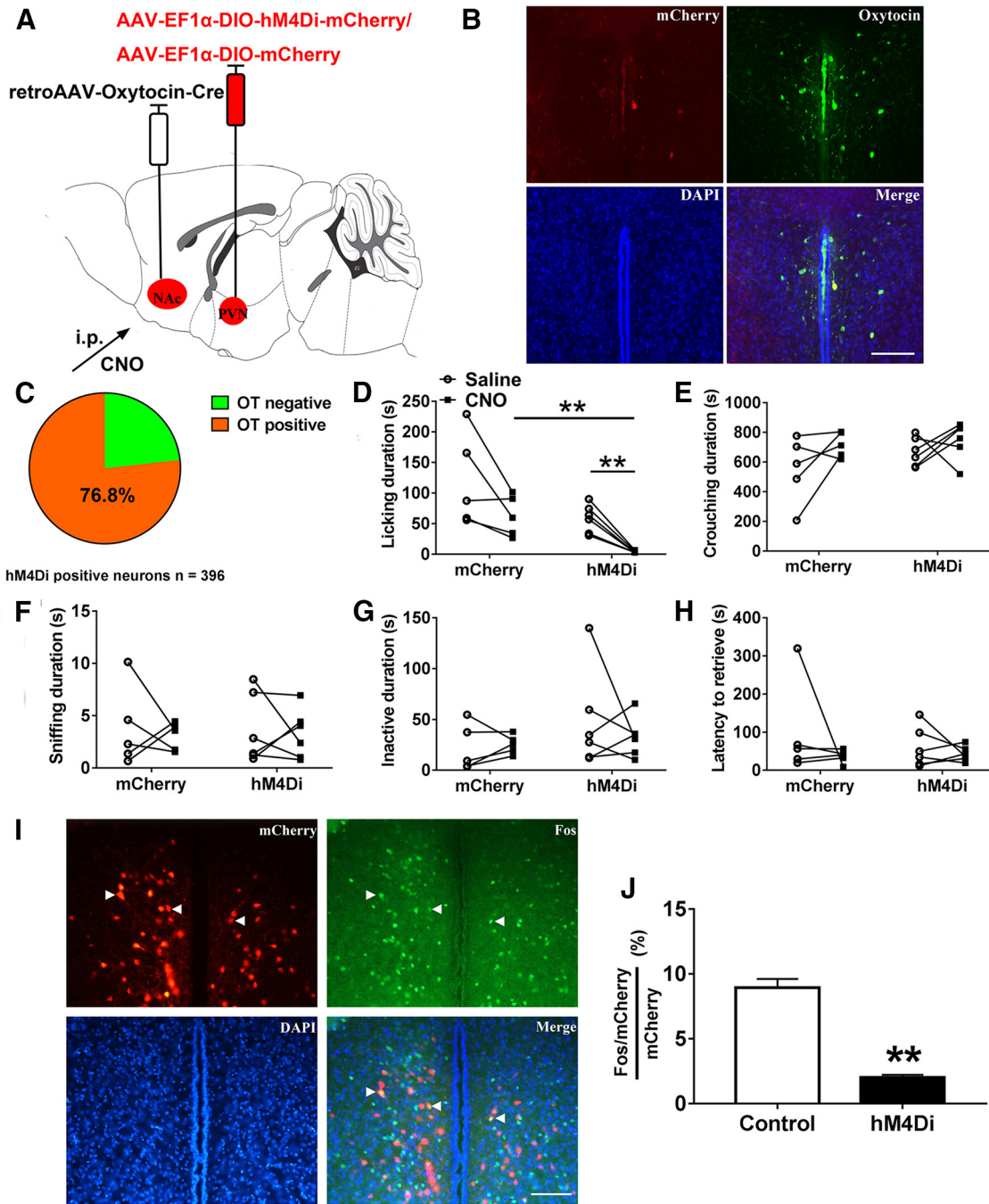
Figure 9. Chemogenetic inhibition of the PVN to NAc OT pathways suppresses paternal behaviors. **A**, Viral strategy. **B**, Co-localization of hM4Di expression (red), OT immunoreactivity (green), and DAPI (blue) in the PVN. Scale bar: 100 μm. **C**, Statistical chart showed that hM4Di-mCherry was relatively restricted to OT-positive cells ($n = 2$). **D–H**, Effect of inhibition of PVN to NAc OT pathways on the duration of (**D**) licking/grooming (interaction: $F_{(1,9)} = 0.011$, $p = 0.920$; treatment: $F_{(1,9)} = 19.826$, $p = 0.002$, $t_{(5)} = 6.087$, $p = 0.002$; group: $F_{(1,9)} = 7.903$, $p = 0.020$, $t_{(9)} = 4.366$, $p = 0.017$), (**E**) crouching (interaction: $F_{(1,9)} = 0.431$, $p = 0.528$; treatment: $F_{(1,9)} = 3.697$, $p = 0.087$; group: $F_{(1,9)} = 1.719$, $p = 0.222$), (**F**) sniffing pups (interaction: $F_{(1,9)} = 0.024$, $p = 0.881$; treatment: $F_{(1,9)} = 0.270$, $p = 0.616$; group: $F_{(1,9)} = 0.001$, $p = 0.973$), (**G**) inactivity (interaction: $F_{(1,9)} = 0.616$, $p = 0.453$; treatment: $F_{(1,9)} = 0.238$, $p = 0.637$; group: $F_{(1,9)} = 1.510$, $p = 0.250$), and (**H**) the latency to retrieve a pup (interaction: $F_{(1,9)} = 0.567$, $p = 0.471$; treatment: $F_{(1,9)} = 1.640$, $p = 0.232$; group: $F_{(1,9)} = 0.369$, $p = 0.559$). mCherry ($n = 5$), hM4Di-mCherry ($n = 6$). Two-way ANOVA with for repeated measures; **$p < 0.01$. Data are mean $\pm$ SEM. **I**, Representative images of the PVN illustrating Fos in neurons expressing mCherry. Scale bar: 100 μm. **J**, Percentage mCherry neurons in the PVN expressing Fos after CNO injection ($t_{(4)} = 9.926$, $p = 0.001$; $n = 3$). Independent t test; **$p < 0.01$. Data are mean $\pm$ SEM.

CNO-treatments decreased pup licking compared with saline treatments in hM4Di-mCherry (inhibitory) fathers ($p = 0.002$) but not in mCherry (control) fathers (Fig. 9D). hM4Di-mCherry fathers spent less time licking and grooming their pup than mCherry fathers after CNO injection ($p = 0.002$), whereas the total duration of pup licking was not affected by saline injection (Fig. 9D). We observed no change in crouching (Fig. 9E), sniffing (Fig. 9F), inactivity (Fig. 9G), or the latency to retrieve a pup (Fig. 9H) following inhibition of the PVN to NAc OT circuit. Compared with the control group, the percentages of mCherry neurons co-expressing Fos were significantly lower in hM3Dq group after CNO administration ($p = 0.001$; Fig. 9I,J) validating the efficacy of chemogenetic inhibition.

Discussion

Our current understanding of the neural mechanism underlying paternal care remains limited. Recently a role for galanin circuits originating in medial preoptic areas in inhibiting C57 mice infanticide and facilitating paternal care has been established (Wu et al., 2014; Kohl et al., 2018). In this study, we used multidisciplinary techniques to explore the neural circuits underlying paternal care using monogamous mandarin voles and found that PVN-VTA OT projections/VTA-NAc DA projections and PVN-NAc OT projections regulate active paternal nurturing behavior, specifically licking and grooming.

Our study provides first evidence that PVN-VTA OT projections modulate paternal care. The data in the present study indicate that chemogenetic activation/inhibition of the PVN (OTergic)-VTA pathway increased/reduced licking and grooming of pups by fathers. The PVN-VTA circuit promotes active paternal care. The current result is supported by one previous study that OT fibers in the VTA originate from PVN OT neurons and OT receptors (OTRs) are located on both DAergic and GABAergic neurons in C57 mice (Xiao et al., 2017). OT enhances the excitability of a specific population of VTA DA neurons that increase DA release in the NAc of C57 mice and gates social reward (Hung et al., 2017). However, a C57 mouse model relevant to autism (*Nlgn3*-knock-out) has impaired social behavior and impaired OT responses in VTA DA neurons (Hörnberg et al., 2020). Infusion of OT directly into the VTA restores social behavior and increases DA release in the NAc shell of Long–Evans rats (Shahrokh et al., 2010). Similarly, injection of OT antagonist into the VTA impaired the postpartum onset of Sprague Dawley rat maternal behavior (Pedersen et al., 1994). Our results using *in vivo* fiber photometry to measure changes in DA release during paternal care found that DA release increased significantly during paternal care and inhibition of PVN-VTA OT projections reduced NAc DA release during active paternal nurturing. This finding provides new evidence that PVN-VTA OT projection regulates paternal care via alteration of DA release. Consistent with infusion of OT into the VTA increased the DA signal in the NAc of Long–Evans rats (Shahrokh et al., 2010). The mechanisms that PVN-VTA OT circuits regulate parental care may be conserved between two sexes. Previous studies indicated that MPOA galanin neurons of C57 mice were activated during parenting in both sexes (Wu et al., 2014), the anteroventral periventricular nucleus TH neurons were critical for maternal care, while the equivalent neurons had no effect on parental behavior in CD-1 male mice but rather suppresses aggression (Scott et al., 2015). Maternal behavior is clearly influenced by profound peripartum hormonal levels (estrogen, progesterone, and prolactin; Kohl and Dulac, 2018). Similarly, virgin CF-1 house male mice undergo a pup-directed aggression to paternal behavior transition after mating (vom Saal, 1985). However, chemogenetic activation of PVN to VTA OT inputs produced no effect on DA signals in the NAc in the present study. This might be because of the fact that interacting with pups increases DA to optimal levels and further chemogenetic activation of the PVN (OTergic)-VTA pathway could not further increase DA release in the NAc because of a "ceiling effect." We also revealed that PVN-VTA OT neurons were activated on eating carrot. Furthermore, chemogenetic inhibition of PVN-VTA OT projections decreased DA release in fathers on eating carrot. This finding is consistent with previous studies that PVN OT neurons are activated on feeding in Sprague Dawley rats (Kohno et al., 2008) and New Zealand White rabbits (Caba et al., 2020). However, some studies found that exogenous OT injection in the VTA

suppressed food intake in Wistar rats (Mullis et al., 2013) and Sprague Dawley rats (Wald et al., 2020). In the PVN, OT neurons may play an important role in an entraining signal for food synchronization to control metabolic homeostasis (Onaka and Takayanagi, 2019; Caba et al., 2020). In the future, the relation of OT circuits and food intake requires further study. These results suggest that this circuit may be involved in the reward-related stimuli of both food and social reward.

Given the involvement of PVN-VTA OT projections in active paternal care, we wondered whether VTA-NAc DA projections regulate active paternal care. Although ~30–40% of VTA-targeted cells are not TH-positive neurons, we found that optogenetic activation/inhibition of the VTA inputs to NAc increased/decreased active paternal behavior (licking and grooming), respectively, suggesting a possible role of the VTA to NAc DA pathway in the control of the motivational aspects of paternal behavior. This finding is consistent with a previous report that Long–Evans hooded rat dams increased DA release in the NAc during periods of pup licking and grooming, and the DA signal in the NAc shell was significantly greater during mother-pup interactions in high, compared with low, licking/grooming mothers (Champagne et al., 2004). The stimulation of the VTA DA neurons projecting to the NAc inhibits NAc GABAergic input to the ventral pallidum, causing maternal behavior (Numan and Stolzenberg, 2009; Olazábal et al., 2013; Numan and Young, 2016). Optogenetic stimulation of VTA-originating DA terminals in the NAc of C57 mice also increases social interaction (Gunaydin et al., 2014). These reports support our findings that VTA-NAc DA projection may reinforce paternal behaviors.

Previous studies found that PVN OT neurons in prairie voles also project to the NAc directly (Ross et al., 2009). Whether this pathway is involved in paternal care was also investigated in the present study. In this experiment, we found that activation of PVN to NAc OT neurons increased the duration of licking/grooming, and decreased the latency to retrieve pups. Inactivation of PVN to NAc OTergic projections reduced the duration of licking/grooming for pups. This result is consistent with previous findings that pup exposure increased the number of OT-immunoreactive cells in the PVN in virgin male prairie voles (Kenkel et al., 2012). Moreover, prairie vole fathers have more OT-positive neurons in the PVN than virgin males (Kenkel et al., 2014), indicating that pup exposure can be a potent stimulus to the brain OT system. Additionally, OT release in the NAc promotes affiliative social behavior, such as social reward in C57 mice (Dölen et al., 2013; Nardou et al., 2019), pair bonding in prairie voles (Young and Wang, 2004) and maternal behavior in Long–Evans rats (Shahrokh et al., 2010). A key example is OT release into the NAc, which promotes affiliative social behavior. We provide convincing evidence that OT signaling in the NAc also enhances paternal behaviors, potentially by increasing the rewarding aspect of active pup engagement. Activation of PVN to NAc OT neurons is known to increase OT release in the NAc of C57 mice (Nardou et al., 2019). OT exerts biological function via binding to OTRs (Jurek and Neumann, 2018). Monogamous prairie voles have higher OTR density in the NAc compared with rats or mice (Olazábal and Young, 2006b) and blocking NAc signaling in the NAc pharmacologically or using RNA interference impairs alloparental behavior (Olazábal and Young, 2006a; Keebaugh et al., 2015). OTR and DA 2-type receptor interactions may exist in the NAc for regulating affiliative social behavior (Liu and Wang, 2003; Romero-Fernandez et al., 2013; Numan and Young, 2016). We speculate

that the PVN-NAc OTergic pathway enhances paternal motivation by modulating the rewarding properties of pup interactions, but the hypothesis requires further investigation. We also found that PVN to NAc OT neurons were not activated by non-social stimuli, such as selfgrooming, sniffing object and eating carrot, but activated by pups, we speculate that this circuit may be specific for social reward.

However, inhibition of PVN-VTA OT projections and PVN-NAc OT projections did not affect the latency to retrieve a pup while activation these two projections reduced latency to retrieve a pup. This discrepancy may result from the different infection rate between the hM4Di virus (PVN-VTA OT projections: 81.6%; PVN-NAc OT pathway: 76.8%) and hM3Dq-mCherry virus (PVN-VTA OT projections: 93.8%; PVN-NAc OT pathway: 93.2%), it is also possible that stimulation of these pathways is sufficient, but not necessary, for paternal retrieval behavior. Regardless, we show that chemogenetic inhibition of PVN to VTA OT circuits reduced active paternal behavior via reducing VTA-NAc DA signaling and that inhibition of PVN to NAc OT projections also suppressed active paternal nurturing. These findings reveal new aspects to the neuronal circuitry underlying paternal care and provide novel neuronal mechanisms potentially involved in the pathology of abnormal paternal behaviors and its related psychological consequences, such as paternal postpartum depression, paternal abuse and neglecting. Therapeutic strategies targeting these circuits may be effective at treating pathologies associated with impaired paternal responsiveness. The NAc is involved in reward as well as aversion (Klawonn and Malenka, 2018). DA terminals encode aversion in the ventral NAc medial shell and reward in the lateral NAc of C57 mice (de Jong et al., 2019). In the future, it will be important to investigate the relation of DA release in the ventral NAc medial shell or the lateral NAc and active paternal behavior. In addition, it will be important whether other OT neural circuits such as OT projection to mPFC affect paternal behavior. The development of novel tools for manipulating OTR neurons in voles, such as viral-mediated CRISPR and CRISPR generated OTR-Cre and OTR knockout voles in addition to the approaches used here, will enhance our ability to dissect the neural circuitry of social behaviors not typically expressed in traditional laboratory animal models (Horie et al., 2019, 2020; Boender and Young, 2020).

References

Ahern TH, Young LJ (2009) The impact of early life family structure on adult social attachment, alloparental behavior, and the neuropeptide systems regulating affiliative behaviors in the monogamous prairie vole (*Microtus ochrogaster*). Front Behav Neurosci 3:17.

Ahern TH, Hammock EA, Young LJ (2011) Parental division of labor, coordination, and the effects of family structure on parenting in monogamous prairie voles (*Microtus ochrogaster*). Dev Psychobiol 53:118–131.

Bartz JA (2016) Oxytocin and the pharmacological dissection of affiliation. Curr Dir Psychol Sci 25:104–110.

Bhatti P, Delaney T, Poulin M, Hahn-Holbrook J (2019) Oxytocin receptor gene (OXTR) and father support interact to predict depressive symptoms postpartum. Biol Psychol 147:107686.

Boender AJ, Young LJ (2020) Oxytocin, vasopressin and social behavior in the age of genome editing: a comparative perspective. Horm Behav 124:104780.

Caba M, Huerta C, Meza E, Hernández M, Rovirosa-Hernández MJ (2020) Oxytocinergic cells of the hypothalamic paraventricular nucleus are involved in food entrainment. Front Neurosci 14:49.

Champagne FA, Chretien P, Stevenson CW, Zhang TY, Gratton A, Meaney MJ (2004) Variations in nucleus accumbens dopamine associated with individual differences in maternal behavior in the rat. J Neurosci 24:4113–4123.

de Jong JW, Afjei SA, Dorocic IP, Peck JR, Liu C, Kim CK, Tian L, Deisseroth K, Lammel S (2019) A neural circuit mechanism for encoding aversive stimuli in the mesolimbic dopamine system. Neuron 101:133–151.

Dölen G, Darvishzadeh A, Huang KW, Malenka RC (2013) Social reward requires coordinated activity of nucleus accumbens oxytocin and serotonin. Nature 501:179–184.

Dulac C, O'Connell LA, Wu Z (2014) Neural control of maternal and paternal behaviors. Science 345:765–770.

Fang YY, Yamaguchi T, Song SC, Tritsch NX, Lin DY (2018) A hypothalamic midbrain pathway essential for driving maternal behaviors. Neuron 98:192–207.

Gregory R, Cheng H, Rupp HA, Sengelaub DR, Heiman JR (2015) Oxytocin increases VTA activation to infant and sexual stimuli in nulliparous and postpartum women. Horm Behav 69:82–88.

Gunaydin LA, Grosenick L, Finkelstein JC, Kauvar IV, Fenno LE, Adhikari A, Lammel S, Mirzabekov JJ, Airan RD, Zalocusky KA, Tye KM, Anikeeva P, Malenka RC, Deisseroth K (2014) Natural neural projection dynamics underlying social behavior. Cell 157:1535–1551.

He ZX, Young L, Ma XM, Guo QQ, Wang LM, Yang Y, Luo L, Yuan W, Li LF, Zhang J, Hou WJ, Qiao H, Jia R, Tai FD (2019) Increased anxiety and decreased sociability induced by paternal deprivation involve the PVN-PrL OTergic pathway. Elife 8:e44026.

Horie K, Inoue K, Suzuki S, Adachi S, Yada S, Hirayama T, Hidema S, Young LJ, Nishimori K (2019) Oxytocin receptor knockout prairie voles generated by CRISPR/Cas9 editing show reduced preference for social novelty and exaggerated repetitive behaviors. Horm Behav 111:60–69.

Horie K, Inoue K, Nishimori K, Young LJ (2020) Investigation of Oxtr-expressing neurons projecting to nucleus accumbens using Oxtr-ires-Cre knock-in prairie voles (*Microtus ochrogaster*). Neuroscience 448:312–324.

Hörnberg H, Pérez-Garci E, Schreiner D, Hatstatt-Burklé L, Magara F, Baudouin S, Matter A, Nacro K, Pecho-Vrieseling E, Scheiffele P (2020) Rescue of oxytocin response and social behaviour in a mouse model of autism. Nature 584:252–256.

Hung LW, Neuner S, Polepalli JS, Beier KT, Wright M, Walsh JJ, Lewis EM, Luo LQ, Deisseroth K, Dölen G, Malenka RC (2017) Gating of social reward by oxytocin in the ventral tegmental area. Science 357:1406–1411.

Jurek B, Neumann ID (2018) The oxytocin receptor: from intracellular signaling to behavior. Physiol Rev 98:1805–1908.

Keebaugh AC, Young LJ (2011) Increasing oxytocin receptor expression in the nucleus accumbens of pre-pubertal female prairie voles enhances alloparental responsiveness and partner preference formation as adults. Horm Behav 60:498–504.

Keebaugh AC, Barrett CE, Laprairie JL, Jenkins JJ, Young LJ (2015) RNAi knockdown of oxytocin receptor in the nucleus accumbens inhibits social attachment and parental care in monogamous female prairie voles. Soc Neurosci 10:561–570.

Keer SE, Stern JM (1999) Dopamine receptor blockade in the nucleus accumbens inhibits maternal retrieval and licking, but enhances nursing behavior in lactating rats. Physiol Behav 67:659–669.

Kenkel WM, Paredes J, Yee JR, Pournajafi-Nazarloo H, Bales KL, Carter CS (2012) Neuroendocrine and behavioural responses to exposure to an infant in male prairie voles. J Neuroendocrinol 24:874–886.

Kenkel WM, Suboc G, Carter CS (2014) Autonomic, behavioral and neuroendocrine correlates of paternal behavior in male prairie voles. Physiol Behav 128:252–259.

Klawonn AM, Malenka RC (2018) Nucleus accumbens modulation in reward and aversion. Cold Spring Harb Symp Quant Biol 83:119–129.

Kleiman DG, Malcolm J (1981) The evolution of male parental investment in mammals, parental care in mammals (Gubernick DJ, Klopfer PH, eds), pp 347–387. Baltimore: Plenum Publishing Corporation.

Kohl J, Dulac C (2018) Neural control of parental behaviors. Curr Opin Neurobiol 49:116–122.

Kohl J, Babayan BM, Rubinstein ND, Autry AE, Marin-Rodriguez B, Kapoor V, Miyamishi K, Zweifel LS, Luo LQ, Uchida N, Dulac C (2018) Functional circuit architecture underlying parental behaviour. Nature 556:326–331.

Kohno D, Nakata M, Maejima Y, Shimizu H, Sedbazar U, Yoshida N, Dezaki K, Onaka T, Mori M, Yada T (2008) Nesfatin-1 neurons in paraventricular and supraoptic nuclei of the rat hypothalamus coexpress oxytocin and vasopressin and are activated by refeeding. Endocrinology 149:1295–1301.

Li T, Chen X, Mascaro J, Haroon E, Rilling JK (2017) Intranasal oxytocin, but not vasopressin, augments neural responses to toddlers in human fathers. Horm Behav 93:193–202.

Li Y, Zhong WX, Wang DQ, Feng QR, Liu ZX, Zhou JF, Jia CY, Hu F, Zeng JW, Guo QC, Fu L, Luo MM (2016) Serotonin neurons in the dorsal raphe nucleus encode reward signals. Nat Commun 7:10503.

Liu Y, Wang ZX (2003) Nucleus accumbens oxytocin and dopamine interact to regulate pair bond formation in female prairie voles. Neuroscience 121:537–544.

Marlin BJ, Mitre M, D'amour JA, Chao MV, Froemke RC (2015) Oxytocin enables maternal behaviour by balancing cortical inhibition. Nature 520:499–504.

Mascaro JS, Hackett PD, Rilling JK (2014) Differential neural responses to child and sexual stimuli in human fathers and non-fathers and their hormonal correlates. Psychoneuroendocrinology 46:153–163.

Maynard KR, Hobbs JW, Phan BN, Gupta A, Rajpurohit S, Williams C, Rajpurohit A, Shin JH, Jaffe AE, Martinowich K (2018) BDNF-TrkB signaling in oxytocin neurons contributes to maternal behavior. Elife 7: e33676.

Mullis K, Kay K, Williams DL (2013) Oxytocin action in the ventral tegmental area affects sucrose intake. Brain Res 1513:85–91.

Nardou R, Lewis EM, Rothhaas R, Xu R, Yang AM, Boyden E, Dölen G (2019) Oxytocin-dependent reopening of a social reward learning critical period with MDMA. Nature 569:116–120.

Numan M (2007) Motivational systems and the neural circuitry of maternal behavior in the rat. Dev Psychobiol 49:12–21.

Numan M, Stolzenberg DS (2009) Medial preoptic area interactions with dopamine neural systems in the control of the onset and maintenance of maternal behavior in rats. Front Neuroendocrinol 30:46–64.

Numan M, Young LJ (2016) Neural mechanisms of mother-infant bonding and pair bonding: similarities, differences, and broader implications. Horm Behav 77:98–112.

Numan M, Numan MJ, Pliakou N, Stolzenberg DS, Mullins OJ, Murphy JM, Smith CD (2005) The effects of D1 or D2 dopamine receptor antagonism in the medial preoptic area, ventral pallidum, or nucleus accumbens on the maternal retrieval response and other aspects of maternal behavior in rats. Behav Neurosci 119:1588–1604.

Numan M, Stolzenberg DS, Dellevigne AA, Correnti CM, Numan MJ (2009) Temporary inactivation of ventral tegmental area neurons with either muscimol or baclofen reversibly disrupts maternal behavior in rats through different underlying mechanisms. Behav Neurosci 123:740–751.

Olazábal DE, Young LJ (2006a) Oxytocin receptors in the nucleus accumbens facilitate "spontaneous" maternal behavior in adult female prairie voles. Neuroscience 141:559–568.

Olazábal DE, Young LJ (2006b) Species and individual differences in juvenile female alloparental care are associated with oxytocin receptor density in the striatum and the lateral septum. Horm Behav 49:681–687.

Olazábal DE, Pereira M, Agrati D, Ferreira A, Fleming AS, Gonzalez-Mariscal G, Levy F, Lucion AB, Morrell JI, Numan M, Uriarte N (2013) Flexibility and adaptation of the neural substrate that supports maternal behavior in mammals. Neurosci Biobehav Rev 37:1875–1892.

Onaka T, Takayanagi Y (2019) Role of oxytocin in the control of stress and food intake. J Neuroendocrinol 31:e12700.

Patriarchi T, Cho JR, Merten K, Howe MW, Marley A, Xiong WH, Folk RW, Broussard GJ, Liang RQ, Jang MJ, Zhong HN, Dombeck D, von Zastrow M, Nimmerjahn A, Gradinaru V, Williams JT, Tian L (2018) Ultrafast neuronal imaging of dopamine dynamics with designed genetically encoded sensors. Science 360:eaat4422.

Pedersen CA, Caldwell JD, Walker C, Ayers G, Mason GA (1994) Oxytocin activates the postpartum onset of rat maternal behavior in the ventral tegmental and medial preoptic areas. Behav Neurosci 108:1163–1171.

Rilling JK, Young LJ (2014) The biology of mammalian parenting and its effect on offspring social development. Science 345:771–776.

Romero-Fernandez W, Borroto-Escuela DO, Agnati LF, Fuxe K (2013) Evidence for the existence of dopamine D2-oxytocin receptor heteromers in the ventral and dorsal striatum with facilitatory receptor-receptor interactions. Mol Psychiatry 18:849–850.

Ross HE, Cole CD, Smith Y, Neumann ID, Landgraf R, Murphy AZ, Young LJ (2009) Characterization of the oxytocin system regulating affiliative behavior in female prairie voles. Neuroscience 162:892–903.

Scott N, Prigge M, Yizhar O, Kimchi T (2015) A sexually dimorphic hypothalamic circuit controls maternal care and oxytocin secretion. Nature 525:519–522.

Shahrokh DK, Zhang TY, Diorio J, Gratton A, Meaney MJ (2010) Oxytocin-dopamine interactions mediate variations in maternal behavior in the rat. Endocrinology 151:2276–2286.

Tai FD, Wang TZ (2001) Social organization of mandarin voles in burrow system. Acta Theriologica Sinica 21:50–56.

Tai FD, Wang TZ, Zhao YJ (2001) Mating system of mandarin vole (*Lasiopodomys mandarinus*). Acta Zoologica Sinica 47:260–267.

Tang Y, Benusiglio D, Lefevre A, Hilfiger L, Althammer F, Bludau A, Hagiwara D, Baudon A, Darbon P, Schimmer J, Kirchner MK, Roy RK, Wang S, Eliava M, Wagner S, Oberhuber M, Conzelmann KK, Schwarz M, Stern JE, Leng G, et al. (2020) Social touch promotes interfemale communication via activation of parvocellular oxytocin neurons. Nat Neurosci 23:1125–1137.

vom Saal FS (1985) Time-contingent change in infanticide and parental behavior induced by ejaculation in male mice. Physiol Behav 34:7–15.

Wald HS, Chandra A, Kalluri A, Ong ZY, Hayes MR, Grill HJ (2020) NTS and VTA oxytocin reduces food motivation and food seeking. Am J Physiol Regul Integr Comp Physiol 319:R673–R683.

Walum H, Young LJ (2018) The neural mechanisms and circuitry of the pair bond. Nat Rev Neurosci 19:643–654.

Weisman O, Zagoory-Sharon O, Feldman R (2012) Oxytocin administration to parent enhances infant physiological and behavioral readiness for social engagement. Biol Psychiatry 72:982–989.

Wu Z, Autry AE, Bergan JF, Watabe-Uchida M, Dulac CG (2014) Galanin neurons in the medial preoptic area govern parental behaviour. Nature 509:325–330.

Xiao L, Priest MF, Nasenbeny J, Lu T, Kozorovitskiy Y (2017) Biased oxytocinergic modulation of midbrain dopamine systems. Neuron 95:368–384.

Yang HB, de Jong JW, Tak Y, Peck J, Bateup HS, Lammel S (2018) Nucleus accumbens subnuclei regulate motivated behavior via direct inhibition and disinhibition of VTA dopamine subpopulations. Neuron 97:434–449.

Young LJ, Wang Z (2004) The neurobiology of pair bonding. Nat Neurosci 7:1048–1054.

Yuan W, He ZX, Hou WJ, Wang LM, Li LF, Zhang J, Yang Y, Jia R, Qiao H, Tai FD (2019) Role of oxytocin in the medial preoptic area (MPOA) in the modulation of paternal behavior in mandarin voles. Horm Behav 110:46–55.